



An approach to inform air quality management through receptor source apportionment and thermodynamic modelling of fine particulate matter in Red Deer, Alberta, Canada



Yayne-abeba Aklilu^{a,*}, Cristen Adams^b, Gregory R. Wentworth^a, Maxwell Mazur^c, Ewa Dabek-Zlotorzynska^d

^a Alberta Environment and Parks, Resource Stewardship, Airshed Sciences, Edmonton T5J 5C6, Canada

^b Environmental Protection Branch, Environment and Climate Change Canada, Government of Canada, Canada

^c Alberta Environment and Parks, Policy, Ambient Air Policy, Edmonton T5K 2J6, Canada

^d Air Quality Research Division, Science and Technology Branch, Environment and Climate Change Canada, Ottawa, Ontario K1V1C7, Canada

ARTICLE INFO

Keywords:

Source apportionment
Spring
Nitrate
Nitric acid limited
 $\text{PM}_{2.5}$

ABSTRACT

Fine particulate matter ($\text{PM}_{2.5}$) concentrations in Red Deer, Alberta, Canada, exceeded the national Canadian Ambient Air Quality Standards (CAAQS) for 2011–2013. In response, a monitoring campaign was deployed to measure $\text{PM}_{2.5}$ composition and precursor gases. The objective of the study was to assess $\text{PM}_{2.5}$ sources, and ultimately to support management actions to improve air quality. The elevated $\text{PM}_{2.5}$ concentrations were regional scale events, with similar and correlated concentrations observed at two stations in Red Deer, and at a site located 9.4 km upwind. Receptor source apportionment identified 9 factors, with secondary organics/aged smoke, sulphate and nitrate factors making up 60% of the $\text{PM}_{2.5}$ mass. When wildfire-impacted samples are removed, seasonal average $\text{PM}_{2.5}$ mass concentrations are largest in the spring, and are dominated by the sulphate and nitrate factors (74%). The relationship between the sulphate factor and meteorological conditions is consistent with a regional source, which could include the coal-fired power plants and the smaller upstream oil and gas operations in the area. Alberta's power plants are switching from coal to natural gas, sulphate levels are expected to decrease. The elevated nitrate factors appeared to be affected by local emissions sources that differed at each monitoring site, and could include urban and industrial sources. The elevated nitrate factors occurred under regional meteorological conditions that promote nitrate formation, with higher contributions observed for sample days with relative humidity >65%, temperature between 0 to -10°C , and snow cover. The nitrate factor enhancements support a non-negligible contribution from the heterogeneous reactions forming nitric acid. A thermodynamic analysis showed that the ammonia-sulphate-nitrate system is nitric acid limited for this study, suggesting that decreases in nitrogen oxide precursors would help to manage $\text{PM}_{2.5}$ concentrations. This study demonstrates the complexity of managing $\text{PM}_{2.5}$ concentrations in an urban environment with nearby industrial sources.

1. Introduction

Short and long-term exposure to $\text{PM}_{2.5}$ can cause various health effects, including respiratory and cardiovascular morbidity and mortality (Annesi-Maesano et al., 2007; Health Canada, 2021; Koenig, 2000; Xing et al., 2016). Because $\text{PM}_{2.5}$ causes adverse health effects, many jurisdictions use $\text{PM}_{2.5}$ mass concentrations as an indicator for air quality management, such as the National Ambient Air Quality Standards of the United States Environmental Protection Agency, the National Air

Quality Ambient Standards of China, the Air Quality Standards of European Union, and the Canadian Ambient Air Quality Standards (CAAQS).

When an air quality standard is approached or exceeded, an investigation is typically launched to determine the causes of the air quality issue (Gulia et al., 2015). Analytical tools such as Positive Matrix Factorization (PMF) can be applied to $\text{PM}_{2.5}$ composition data to provide insight into the source type and origin of $\text{PM}_{2.5}$ (Belis et al., 2013; Brown et al., 2015; Hopke, 2016) and has been successfully used in areas of

* Corresponding author.

E-mail address: yayne-abeba.aklilu@gov.ab.ca (Y.-a. Aklilu).

complex emission sources (e.g., Cropper et al., 2019; Dai et al., 2020; Jeong et al., 2016; Lee et al., 2008; Al Mamun et al., 2021). Thermodynamic modelling can also be used to assess the sensitivity of inorganic secondary PM_{2.5} mass concentrations to changes in precursor levels and/or meteorology. For example, the Extended-Aerosol Inorganics Model (E-AIM) has been used previously to determine whether aerosol is deliquesced (e.g., Sun et al., 2018) and estimate aerosol pH (e.g., Murphy et al., 2017; Parworth et al., 2017; Tao and Murphy, 2019).

In Canada, PM_{2.5} is managed under the Air Quality Management System under which the CAAQS is the driver (CCME, 2019a). There is a 24-hr standard of 28 µg/m³, which is calculated from the 3-year average of the annual 98th percentile of the daily 24-hr average concentrations. There is also an annual standard of 10 µg/m³, which is calculated the 3-year average of the annual average of the daily 24-hr average concentrations. In Alberta, a province in western Canada, concentrations of PM_{2.5} are affected by a complex set of emissions sources and meteorology. In many regions of the province, PM_{2.5} is at concentrations that are approaching both the 24-hr and annual CAAQS (Brown et al., 2022), primarily due to winter and springtime PM_{2.5} episodes. PM_{2.5} from wildfires is not included in comparison to the CAAQS but can complicate data interpretation and emission source attribution. Wildfire smoke intermittently affects regions across the province, and 1-hr average PM_{2.5} concentrations can exceed 1000 µg/m³ during severe smoke episodes (e.g., Brown, 2021; Landis et al., 2018).

There have been few studies on PM_{2.5} composition in Alberta, and the findings are indicative of the complex sources that can impact air quality. In the oil sands region, sources with sulphur content from large oil upgraders, dust, and wildfire smoke are the largest contributors to PM_{2.5} (Landis et al., 2017; Al Mamun et al., 2021). In Alberta's two largest cities, Edmonton and Calgary, secondary inorganic particulate matter, including ammonium sulphate and nitrate, can make up a substantial fraction of PM_{2.5} outside of the wildfire season (Bari and Kindzierski, 2016, 2017; Dabek-Zlotorzynska et al., 2011; Government of Alberta, 2014). There have been few in-depth studies of particulate matter composition and sources in other areas of the province, and none were explicitly intended to inform air quality management.

In the 2011–2013 CAAQS assessment, PM_{2.5} concentrations exceeded the CAAQS at the Red Deer Riverside station in Alberta, Canada (Government of Alberta, 2015), indicating that action is needed to improve air quality in the region. Red Deer experiences mixed emissions from urban sources as well as surrounding industry, including oil and gas development. Extensive analysis of routine monitoring in Red Deer found that PM_{2.5} composition sampling was needed to provide additional information about emissions source contributions, particularly for secondary PM_{2.5} (Bari and Kindzierski, 2017; Government of Alberta, 2016). Therefore, three PM_{2.5} composition samplers were deployed to the Red Deer area, and data were analyzed to understand the major contributors to elevated PM_{2.5} in Red Deer, Alberta, Canada.

PMF analysis was applied to the composition data in order to attribute sources of PM_{2.5}, and a cluster analysis was used to determine the relationships between PMF source factors and other co-monitored parameters such as trace gas concentrations and meteorology. Since ammonium nitrate is a large component of wintertime particulate matter in parts of Alberta (Bari and Kindzierski, 2016; Government of Alberta, 2014), a thermodynamic sensitivity analysis (Guo et al., 2018) was performed to investigate whether ammonium nitrate is limited by nitric acid (HNO₃) or ammonia (NH₃) and thus identify the more effective emission management strategy. This paper provides a framework for elucidating PM_{2.5} sources and identifying potential management actions that can be applied to similar regions that experience elevated PM_{2.5} levels.

2. Materials and methods

2.1. Study area and emission sources

Red Deer is located in central Alberta, Canada and has a population of approximately 190,000, including surrounding municipalities (Government of Alberta, 2022). Red Deer experiences a cold climate, no dry season, and cool summers (Beck et al., 2018), with daily average temperatures ranging between -10.2 °C in January and 23.1 °C in July, and a persistent snow-pack typically from November until mid-March (Government of Canada, n.d.).

Red Deer experiences mixed air emissions from urban, industrial, agricultural and natural sources, which can affect PM_{2.5} concentrations. These emissions include both primary PM_{2.5} and precursors to secondary PM_{2.5}, including oxides of nitrogen (NO_x), sulphur dioxide (SO₂), volatile organic compounds (VOC), and NH₃. This complicates source attribution when determining appropriate management actions to address the 2011–2013 CAAQS exceedance. Fig. 1 shows a map of the Red Deer area, with major emissions sources of primary PM_{2.5} and precursors indicated, as discussed in the paragraphs below.

Red Deer is affected by typical urban emissions, such as traffic on local roadways and provincial highways, as well as residential and commercial sources. On-road transportation generates gaseous emissions via fuel combustion (May et al., 2014), including NO_x, a precursor to the formation of ammonium nitrate (a type of secondary PM_{2.5}) and VOCs. On-road transportation emits primary particulate through fuel combustion and the mechanical wear of vehicular components, such as brakes and tires (Thorpe and Harrison, 2008). Primary PM_{2.5} is also emitted from salt and sand mixtures applied to roadways during the winter (City of Red Deer, 2022). Many rural roads outside the city are unpaved and are another source of primary particulate matter (dust) in the warmer season when roads are not frozen and are free of snow (Government of Alberta, 2016). Residential heating in Alberta is predominantly provided by the combustion of natural gas (Statistics Canada, 2011), leading to NO_x emissions. Residential wood combustion is primarily recreational (i.e., backyard fire pits, fireplaces) and may be a small contributor to PM_{2.5} and its precursors.

Industrial emissions contribute to NO_x, VOCs and the vast majority of SO₂ in the Red Deer area (Government of Alberta, 2016). Fig. 1 shows the location of large emitters of precursors (primarily NO_x and SO₂) and primary PM_{2.5} in the region (Government of Canada, 2021). In the study area, electric power generation is the highest industrial emitter of primary PM_{2.5}, SO₂ and NO_x, followed by upstream oil and gas facilities (Table A1 in Supplemental Information). Upstream oil and gas facilities, ubiquitous in the area, are the highest contributors of VOCs. Speciated VOCs information for the area are limited to large downwind oil and gas facilities such as petrochemical industries. Within the city of Red Deer, industrial sources include facilities related to incineration and waste, manufacturing and commercial and institutional sectors. Immediately northeast of Red Deer, there are manufacturing facilities. The more distant large coal-fired power plants made up 72% of the SO₂ emissions (Table A1 in Supplemental Information). Coal-fired power generation is being phased out in Alberta and replaced largely with natural gas-fired (Government of Alberta, 2018); coal-fired power generation fell from 26% of the power produced in Alberta in 2017 to 19% in 2019, and as of 2022, this has decreased to 8% (Alberta Electric System Operator, 2022).

The Red Deer River runs north-easterly through the city, within river valleys and hummocky terrain, which supports mixed forests and uncultivated grassland. Biogenic activity can result in primary particulate matter emissions such as spores, pollen, or plant debris, although these emissions are predominantly in the coarse fraction (i.e., 2.5 µm < PM < 10 µm) (Bauer et al., 2008; Samaké et al., 2019), evidence of biogenic particulate matter have been observed in PM_{2.5} (Liang et al., 2013). In addition, the city is surrounded primarily by agricultural lands, which can be a source of dust and ammonia. Red Deer also experiences

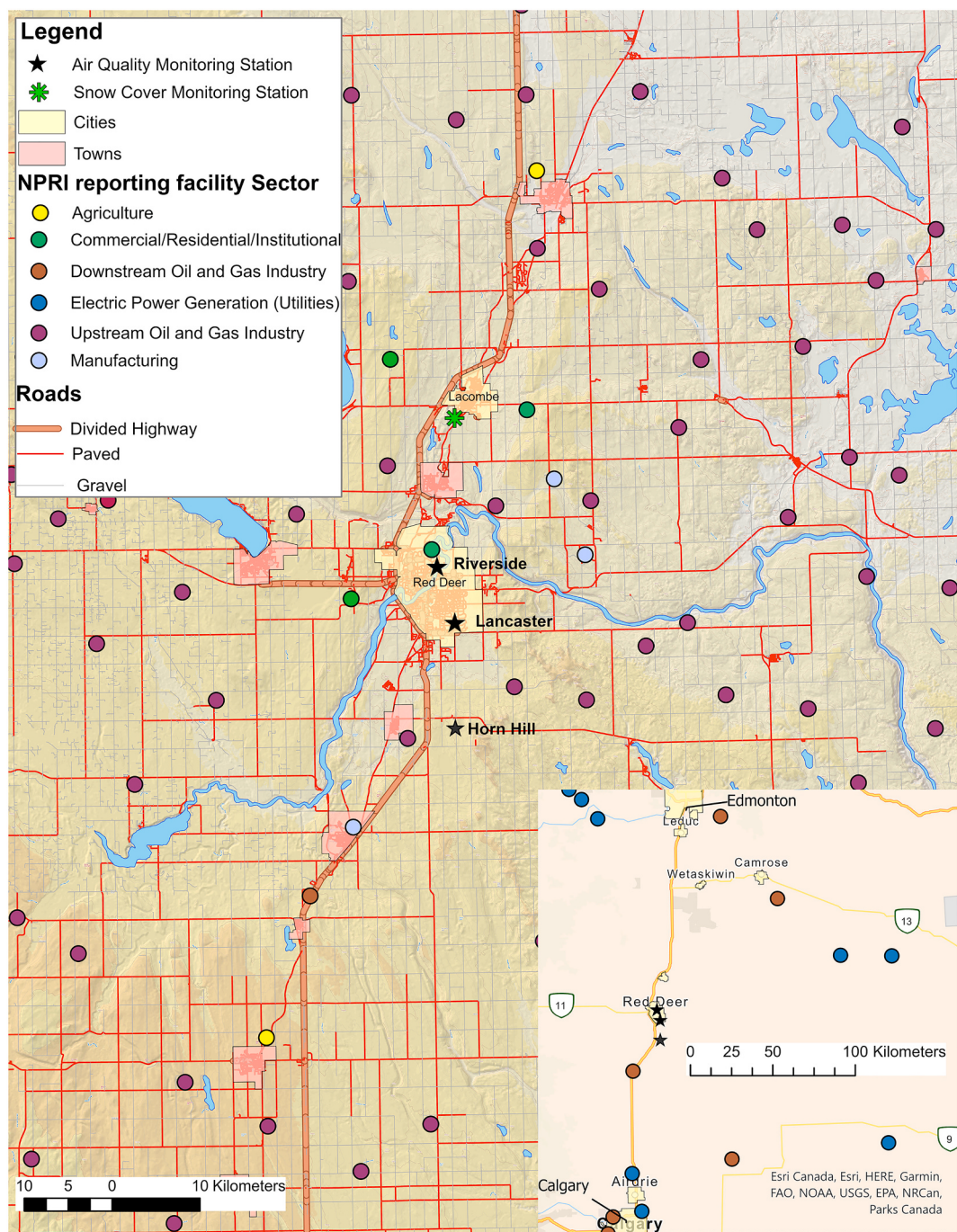


Fig. 1. Map of the Red Deer study area with locations of monitoring stations, population centres, and 2018 NPRI-reporting emissions sources (Government of Canada, 2021c). Inset: Surrounding area, with Electric Power Generation and Downstream oil and gas NPRI-reporting emissions sources indicated, other sectors indicated on the main map are not included in the inset but are abundant. The base map was provided by Topographic Data of Canada - CanVec Series (<https://open.canada.ca/data/en/dataset/>). (For interpretation of the references to colour in this figure legend, the reader is referred to the web version of this article.)

intermittent episodes of smoke transported from wildfires, which are most frequently observed from April to August.

2.2. Air quality monitoring

The study monitoring sites include two long-term air monitoring stations in Red Deer (Riverside and Lancaster) and one temporary monitoring station (Horn Hill) located south of Red Deer, as shown in Fig. 1. The Riverside monitoring station ($52^{\circ} 17' 56''$ N and $113^{\circ} 47' 37''$ W; 840 m asl) is located in an industrialized portion of Northeast Red Deer within the Red Deer River valley. The Lancaster monitoring station

($52^{\circ} 14' 27.10''$ N and $113^{\circ} 45' 55.26''$ W; 900 m asl) is located in a residential area of South Red Deer. The Horn Hill station ($113^{\circ} 45' 49.53''$; 955 m asl) was temporarily deployed 9.4 km south of Red Deer to understand upwind air quality and PM_{2.5} composition and is surrounded by cropland away from known NO_x emission sources.

PM_{2.5} mass (measured using Hybrid Nephelometer/Beta Attenuation System (SHARP)) and various gaseous pollutant concentrations were monitored at all three stations. In addition, 24-hr integrated PM_{2.5} mass samples were collected for composition analysis, as described in Sect. 2.3. Table A2 in the Supplemental Information lists the monitored species at the three sites. Snow cover data from the nearest climate station,

located 15 km north of Red Deer (LACOMBE CDA 2 (<https://climate.weather.gc.ca/>) was also used in the analysis.

Predominant wind directions across the region are reasonably consistent, with south-southeast and northwest components that vary little by season. Wind speeds appear to be influenced by elevation, with Riverside station experiencing a larger proportion of lower wind speeds than the more elevated and open sites of Lancaster and Horn Hill. Wind roses for the period of study at the three sites are shown in Fig. A1 in the Supplemental Information.

2.3. Sample collection and PM_{2.5} composition analysis

24-hr integrated samples of PM_{2.5} composition were collected at all three air monitoring stations between February 2017 and March 2019 on a three-day sampling schedule. Deployment of monitoring was staggered at the three monitoring sites. Sample collection was initiated at the Riverside station (location of CAAQS exceedance) on February 18th, 2017 ($n = 260$), at the Horn Hill station (rural site) on October 28th 2017 ($n = 142$), and at the Lancaster station on January 8th 2018 ($n = 176$). Integrated sample collection at all sites ended in March 2019. All three stations integrated data was collected for at least 15 months.

Partisol 2000i samplers (Partisol) and a Met One Super SASS were used to collect the samples. The Partisol was fitted with a Teflon filter, which was used to determine gravitational mass and metals using energy dispersive x-ray fluorescence (ED-XRF), acid digestion and inductively-coupled plasma mass spectrometry (ICP-MS). The Super SASS has three sample flows, each equipped with a sample cartridge (A, B and C). Quartz filter fibres from cartridge A were analyzed for organic carbon (OC) and elemental carbon (EC) using the IMPROVE thermal/optical reflectance (TOR) protocol. OC1–4 were derived at four temperatures ranging from 120 °C and 550 °C; EC1–3 were derived at three temperatures ranging from 550 °C to 800 °C. Cartridge B contained quartz filters, which were used to identify positive OC artefacts; the cartridge also contained a Teflon filter used to collect PM_{2.5} mass. Cartridge C contained two denuders and a Teflon and a nylon filter. Ions were analyzed by ion chromatography (IC) from water extracted Teflon filters. Denuders in Cartridge C were used to collect gaseous NH₃, SO₂, and HNO₃. Extracts from the nylon filter were analyzed for volatile nitrate (NO₃⁻). A detailed description of sample collection and laboratory analysis is found in Dabek-Złotorzynska et al. (2011).

Prior to PMF and thermodynamic modelling analysis, several steps were taken to consolidate and prepare the PM_{2.5} data. PM_{2.5} gravitational mass concentration is determined using samples collected by the Partisol and the SASS. The Partisol mass concentration data had lower detection limits and therefore were used when available. When Partisol mass concentration data were missing, the SASS gravimetric data from Cartridge B were substituted. For the metals and elements that are analyzed by both ICP-MS and ED-XRF, the ICP-MS reported concentrations were used when available. Silicon (Si), bromine (Br), and rubidium (Rb) concentrations were only reported by ED-XRF. The OC was determined by subtracting the OC artefact from Cartridge B from the OC measured from Cartridge A. Volatile NO₃⁻ from the nylon filter of Cartridge C was added to the NO₃⁻ concentrations reported from the Teflon filters.

2.4. Identification of wildfire smoke impact

As part of the annual CAAQS assessment, data collected at select monitoring stations in Alberta, including the Red Deer Riverside and Lancaster stations, are evaluated for wildfire smoke impact using multiple datasets (Brown, 2021; CCME, 2019b). Wildfire impacted days are identified using satellite imagery (<https://worldview.earthdata.nasa.gov>), back trajectories (obtained from Environment Climate Change Canada), maps of past wildfires and smoke forecasts (<https://firesmoke.ca>), PM_{2.5} concentration data from nearby monitoring stations (to identify regional impact), information gathered throughout the year as

part of the Air Quality Health Index and associated air quality advisories, and through communication with station operators. This process identifies wildfire smoke with notable impact on PM_{2.5} samples; marginal impacts may not be recognized.

2.5. PMF analysis

Analytical tools such as receptor modelling are able to take a large matrix of particulate matter component concentration data and its associated uncertainties and decompose it to provide insight into the source type and origin of PM_{2.5}. EPA PMF V5.0 (US-EPA, 2014), with its improved error estimation methods (Brown et al., 2015), was used to identify the most robust PMF solution. An in-depth description of PMF is found elsewhere (e.g., Paatero, 1997).

Speciated PM_{2.5} data at all three stations were pretreated using the recommended methods (US-EPA, 2014). Missing data were replaced with the geometric mean of the compound over the monitoring period at a station. Concentrations below the detection limit were replaced with a value of half the detection limit. For each measurement, the uncertainty was estimated based on the detection limit to generate the uncertainty matrix (US-EPA, 2014).

PMF was initially run for individual stations. All factors, except for one, were comparable between sites, with a coefficient of variance <25%, indicating that the data were suitable for a combined multi-site PMF analysis (Pandolfi et al., 2019). To determine the optimal number of factors for the multi-site PMF analysis, the solutions for 4 to 12 factors were run (Figs. A2–4 in the Supplemental Information). The final matrix for the multi-site PMF analysis contained 31 strong and 18 weak species. Thirteen species were excluded from the analysis. PM_{2.5} mass concentrations were included as a total variable. A time series of these components was examined to ensure meaningful temporal variability. Two sample days, August 15 and August 18, 2018, were excluded from the analysis at all three stations due to poor fit. These two days had extremely high PM_{2.5} concentrations as a result of an extraordinary impact from wildfire smoke (Table A3 and 4 in the Supplemental Information).

A 9 factor solution passed a set of criteria (Table A5 in the Supplemental Information), with resolved factors that were consistent with known emissions sources in the area, no swaps in the Disp test, at least 85% of the bootstrap (BS) sampled matching the base run results in the BS test, and no swaps observed in the BS-Disp test (Table A6 in the Supplemental Information). The apportioned total mass concentrations were comparable to the measured mass concentrations (slope = 1.05, intercept = 0.15 µg/m³ and R² = 0.85).

2.6. Conditional bivariate probability function

A Conditional Bivariate Probability Function (CBPF) (Uria-Tellaetxe and Carslaw, 2014) was used to establish the relationship between the resolved factors, wind speed, and wind direction at the three monitoring sites. Hourly average wind speed and wind direction data were co-monitored at each of the three stations. The timeAverage and polarPlot functions from the R Openair package (Carslaw and Ropkins, 2012) were used to determine 24-hr average wind speed and wind directions for the days that the integrated samples were collected, and to generate CBPF. Wind direction may at times greatly vary throughout the day and 24-hr values may not be fully representative of wind directions observed throughout a 24-hr period. However, the qualitative patterns in the CBPF matches expected sources and the method was useful in resolving regional and local sources. CBPF were generated using available data with concentrations equal to or higher than the 75th percentile, thus illustrating the probability that elevated concentrations would be observed for a given wind sector and speed. The assumption is that for a persistent and notable source, CBPF will illustrate a high probability when the monitoring site is downwind of the source.

2.7. Cluster analysis

A cluster analysis was used to identify associations between factors and other parameters such as gaseous pollutant concentrations and meteorology. The analysis was performed for data collected at Red Deer Riverside station as this site has the longest speciated dataset.

The input to the cluster analysis was a time series of 24-hr averaged variables aligned to the three-day PM_{2.5} sampling schedule. The factor time series were obtained from the PMF analysis. 24-hr integrated samples of NH₃ and HNO₃ were obtained from Met One Super SASS Denuders in Cartridge C. Daily averages of air quality parameters (ozone, H₂S, non-methane hydrocarbons (NMHC), CH₄, NO, NO₂ and SO₂) and meteorology (temperature and relative humidity (RH)) were calculated from hourly data, requiring 75% data completeness. Snow cover data from the nearest climate station 15 km north of Red Deer were classified into categories of 0 cm, < 1 cm, 1–5 cm, 5–10 cm, > 10 cm. Total daily solar radiation was calculated from hourly solar radiation data collected at Lancaster station. The data for each variable included in the cluster analysis were scaled by subtracting the mean and dividing by the standard deviation, using the “scale” function in R ([Core Development Team, 2021](#)). Only days with valid data for all variables were included in the cluster analysis.

The hierarchical clustering method ([Core Development Team, 2021](#)) was used in this analysis. Distance was calculated using the Euclidean method, and clustering was conducted using the Ward2 method. The hierarchical method resolved five clusters. The k means clustering ([Core Development Team, 2021](#)) was also tested, with five clusters specified, and yielded similar results to the hierarchical clustering.

2.8. Thermodynamic modelling

The thermodynamic model E-AIM was used to investigate ammonium nitrate formation, which can be a major component of cold season PM_{2.5} in the region (e.g., [Bari and Kindzierski, 2016](#)). E-AIM is a thermodynamic model used to calculate gas-liquid-solid phase partitioning in aerosol systems at thermodynamic equilibrium ([Wexler and Clegg, 2002](#)). Equilibrium is achieved in E-AIM when the total Gibbs free energy reaches a minimum and is calculated using equations for aqueous phase activity coefficients, as well as gas-liquid and solid-liquid equilibrium constants.

The model is freely accessible online at: <http://www.aim.env.uea.ac.uk/aim/aim.php>. In this work, the Inorganic Model II is used to investigate the partitioning of HNO₃/NO₃⁻ and NH₃/NH₄⁺ ([Clegg et al., 1998](#)). Model inputs include meteorological parameters (i.e., RH, pressure, and temperature) as well as mole loadings of SO₄²⁻, NO₃⁻, HNO₃, ammonium (NH₄⁺), and NH₃ in mol m⁻³ of air from 24-hr integrated samples. Aerosol ion balance is accomplished by inputting sufficient H⁺ or OH⁻ to achieve electroneutrality. The formation of solids and partitioning of NH₃ and HNO₃ were allowed. Pertinent model output included the equilibrium mole loadings of the aforementioned species.

For this study, E-AIM is used to quantify the change in secondary PM_{2.5} ion mass (sum of NH₄⁺, NO₃⁻ and SO₄²⁻) as total ammonium (i.e., NH₃ + NH₄⁺) or total nitrate (i.e., HNO₃ + NO₃⁻) are varied from -25%, -10%, +10%, and + 25% of measured. This approach reveals whether the formation of ammonium nitrate is limited by HNO₃ or NH₃ and quantifies the sensitivity of PM_{2.5} mass to changes in total ammonium and nitrate, which is necessary information to develop effective mitigation strategies.

3. Results and discussions

3.1. Spatial variation of PM_{2.5} and NO₂

The hourly data collected at the study monitoring sites between February 2017 and March 2019 were used to evaluate the spatial variation of PM_{2.5} and other air monitoring parameters. The study mean

concentrations and standard error (σ/\sqrt{N}) were calculated using hours during which valid data for the given parameter was collected at all three monitoring stations. The study mean PM_{2.5} concentrations are comparable at the three stations ($8.5 \pm 0.1 \mu\text{g}/\text{m}^3$ at Riverside, $8.1 \pm 0.1 \mu\text{g}/\text{m}^3$ at Lancaster, and $8.3 \pm 0.1 \mu\text{g}/\text{m}^3$ at Horn Hill). Furthermore, similar temporal variation in PM_{2.5} is observed across the three stations. The Pearson correlation coefficient for data collected at Riverside and Horn Hill, the two most distant stations, is $R = 0.90$. The strong correlation is somewhat influenced by the large peaks in regional PM_{2.5} when wildfire smoke is in the area. However, the PM_{2.5} concentrations at Riverside and Horn Hill are still correlated, $R = 0.77$, when only data from outside wildfire season are considered. Other air quality parameters are not as comparable across stations. For example, larger concentrations of NO₂ are observed at the urban Riverside ($10.0 \pm 0.1 \text{ ppb}$) and Lancaster stations ($9.1 \pm 0.1 \text{ ppb}$) than at the rural Horn Hill location ($3.92 \pm 0.03 \text{ ppb}$). This is expected based on the known NO_x sources local to the monitoring stations. In addition to the urban sources of NO_x, smaller sources exist throughout the region, with the most notable (2905 tonnes/yr) nearfield source, a chemicals manufacturing facility, to the northeast of the study area ([Government of Canada, 2021](#)). This suggests that a large fraction of PM_{2.5} in the area is affected by regional meteorology and/or emissions sources both during and outside wildfire season and that elevated concentrations associated with the CAAQS PM_{2.5} exceedances in the urban centre are regional in nature.

3.2. Factors from multi-site PMF analysis

The 9 factors from the PMF analysis using data collected between February 2017 and March 2019 are summarised in [Table 1](#). For each factor, PMF output provides (1) a factor fingerprint and (2) a time series of a factor's contribution at the monitoring site. The factor fingerprints indicate the apportionment of each species to each factor, as shown in [Fig. 2](#). The key species and minor species apportioned to a factor are identified in [Table 1](#), which in turn may be related to source categories.

[Fig. 3](#) summarises the contributions of the 9 factors to PM_{2.5}. The relative contribution of factors ([Fig. 3a](#)) indicates that the largest contributions to PM_{2.5} came from the secondary organics/aged smoke (24%), nitrate (20%), sulphate (16%), carryover (14%), and crustal (11%) factors. The relative contributions between the three sites were comparable, within $\pm 2\%$ for most factors. At the three stations, the seasonal mean PM_{2.5} concentrations are largest in the spring and summer months, with large contributions from the nitrate factor in the spring and the secondary organics/aged smoke factor in the summertime ([Fig. 3b](#)). When determining CAAQS achievement, wildfire smoke impacted days are excluded from the analysis. When wildfire-impacted samples ([Brown, 2019, 2021](#)) are excluded, on average the nitrate factor constituted 56% of elevated PM_{2.5} concentrations ($> 15 \mu\text{g}/\text{m}^3$) ([Fig. 3c](#)).

The subsections below describe each of the factors. The fingerprint composition, seasonality, consistency across stations, and relationship to winds were explored in order to understand possible source characteristics. The Kruskal-Wallis Rank Sum test in the basic R package ([Core Development Team, 2021](#)) was used to test whether factor contributions differ between the three monitoring sites over the sample period. For most factors, no significant difference ($p > 0.05$) was observed between the three sites, indicating regional origin or notable influence of meso-scale meteorology. This is consistent with the similarity of PM_{2.5} mass measurements between the sites. The road, fresh smoke and biogenic factors were found to have significant differences between stations (p -values < 0.05), which is consistent with the local nature of the sources contributing to these factors. In most cases, CBPF did not show a strong (> 0.7 probability) relationship between elevated concentrations and wind speed and direction. Selected CBPF figures are shown in the subsections below, and the remaining CBPF figures are provided in the Supplemental Information.

Table 1

Summary of the factors and properties resolved through the multi-site PMF analysis for data collected at the three Red Deer study sites between February 2017 and March 2019 (578 combined samples). OC1–4 are organic carbon components derived at four temperatures ranging from 120 °C and 550 °C; EC1–3 are elemental carbon components derived at three temperatures ranging from 550 °C to 800 °C.

| Factor Name | Key species attributed | Minor species attributed | Likely source |
|-------------------------------|--|--|---|
| Secondary organics/aged smoke | oxalate, K, EC1, OC2–4 | formate | Organics, which have undergone oxidation and aged smoke, which has undergone long-range transport. |
| Nitrate | NO ₃ ⁻ , NH ₄ ⁺ | | Secondary formation of PM _{2.5} from NO _x and NH ₃ precursors. |
| Sulphate | NH ₄ ⁺ , SO ₄ ²⁻ | trace metals, elements | Secondary formation of PM _{2.5} from SO ₂ and NH ₃ precursors. |
| Carryover | Na, Cd | Cl, Zn | Likely from fossil fuel combustion, such as urban and/or industrial activities. |
| Crustal matter Road | Si, Al Cu, Fe, Mo | elements Na, Cl | Regional dust Non-exhaust road traffic emissions such as brake wear and road salt and dust. |
| Selenium | Se, oxalate | SO ₄ ²⁻ , NO ₃ ⁻ | Emissions from industry that emits Se and SO ₂ . Typically associated with coal combustion. |
| Biogenic | arabitol, mannitol | OC2–4, EC2–3, SO ₄ ²⁻ , Si, Ca | Primary biogenic origin associated with vegetation, with some contributions from other regional sources (EC, SO ₄ ²⁻ and Si). |
| Fresh smoke | levoglucosan, mannosan, galactosan | OC1 | Fresh smoke from local wood burning or wildfires. Levoglucosan/mannosan of 4.5 and mannosan/galactosan of 3.6 indicates likely softwood combustion. |

3.2.1. Secondary organics/aged smoke

The secondary organics/aged smoke factor includes the key species oxalate, K⁺, and minor contributions from formate, with minimal presence of anhydrosugars (levoglucosan, mannosan and galactosan) (Fig. 2). This is consistent with organics that have undergone oxidation (Cubison et al., 2011; Hennigan et al., 2010) and the long-range transport of smoke most likely from biomass burning.

The secondary organics/aged smoke factor makes up a significant (24%) contribution to total PM_{2.5} mass, with the largest contribution in the summer (Fig. 3b) when wildfire smoke most often affects Alberta. However, the secondary organics/aged smoke factor also contributes a seasonal mean of 1.01 µg/m³ to PM_{2.5} in the winter, likely as a result of oxidation of organics in the presence of OH radicals and other oxidants (Heard et al., 2004; Kroll et al., 2015). The Kruskal-Wallis test found a similar contribution for secondary organics/aged smoke across the three stations, suggesting a regional impact for this factor. The CBPF analysis did not identify a strong association between the secondary organics/aged smoke factor and wind speed and direction (probability <0.2, Fig. A5 in Supplemental information).

The secondary organics/aged smoke factor has significantly larger contributions during known periods of wildfire influence, identified through CAAQS reporting (Brown, 2021). In the summer of 2017, the 24-hr average secondary organics/aged smoke factor contributed 5–20 µg/m³ to PM_{2.5} when smoke was transported from British Columbia over the Red Deer area. In the summer of 2018, when wildfire smoke was

again transported into the region, the 24-hr average secondary organics/aged factor contributed up to 30 µg/m³ to PM_{2.5} and made up most (63–84%) of the 24-hr average PM_{2.5} mass concentration on days impacted by wildfire smoke. Two sample days highly impacted by wildfire smoke (August 15 and August 18, 2018) were excluded from the PMF analysis due to poor fit. Concentrations measured on these days are listed in the Supplemental Information (Table A3).

3.2.2. Nitrate

The nitrate factor contains the key species NO₃⁻ and NH₄⁺, as well as less volatile organic carbon (OC-4), EC and, to a lesser extent, species associated with road de-icing (Na, Cl) (Fig. 2). The nitrate factor makes a notable contribution (20%) to total PM_{2.5}, with the largest seasonal averages at the three sites (1.52–2.43 µg/m³) in winter and spring (Fig. 3b).

The contributions from the nitrate factor are intermittent. During the study period, the highest contribution from the nitrate factor was observed at Riverside on March 12, 2018, with a 24-hr average contribution to total PM_{2.5} reaching 24.8 µg/m³. Smaller 24-hr average episodes, reaching 5–10 µg/m³ were also observed throughout the winter/spring seasons of 2017, 2018, and 2019. These contributions are comparable in magnitude and frequency to the contributions from the secondary organics/aged smoke factor during the summer season.

Fig. 4 illustrates the relationship between the nitrate factor, relative humidity, temperature and wind speed. Elevated concentrations of the nitrate factor were typically observed for temperatures ranges of 0 to -10 °C, relative humidity >65% and low wind speeds (< 8 km/hr). Warming winter temperatures, increasing amount of incoming solar radiation and snow melt are likely related to the increased relative humidity at this time of year (Harpold and Brooks, 2018). Relative humidity >65% is likely high enough for even internally mixed particulates to deliquesce, allowing for aqueous-phase chemistry. Furthermore, ammonium nitrate formation is more favourable at lower temperatures and higher relative humidity (Seinfeld and Pandis, 2016). The lower wind speeds allow for the accumulation of precursor pollutants over the Red Deer area and facilitate chemical reactions leading to particulate matter formation. These observations are similar to Lin et al. (2020), where cold season episodes are nitrate driven, occur in regimes high in NH₄⁺ and contain higher liquid water content.

On average, contributions from the nitrate factor were comparable at all three monitoring sites, with the seasonal mean springtime nitrate factor concentrations of 2.81 µg/m³ at Lancaster, 2.25 µg/m³ at Riverside, and 2.45 µg/m³ at Horn Hill. This does not track directly with study average NO₂ concentrations, which were notably lower at Horn Hill (3.92 ppb) than at Riverside (10 ppb) and Lancaster (9.1 ppb). When including all data, both during and outside of peak episodes, the Kruskal-Wallis test indicated similar contributions and variability across stations, suggesting that the nitrate factor typically has large concentrations at all three stations during air pollution episodes. The regional nature of the nitrate factor could be due to meteorological conditions that promote the accumulation of precursors and the subsequent formation of ammonium nitrate. However, CBPF analysis for nitrate factor points to different source areas for each site (Fig. 5), with higher contributions for low wind speeds (< 5 km/h) at Lancaster, a southerly influence for wind speeds <10 km/h at Riverside, and a southeasterly influence for both lower and higher wind speeds at Horn Hill. This suggests that under certain regional meteorological conditions that promote nitrate formation, the nitrate factor concentrations at individual monitoring sites may be affected by local emissions sources (as in the case of the urban sites) or the variability of precursors upwind (as in the case of Horn Hill).

3.2.3. Sulphate

The sulphate factor includes SO₄²⁻ and NH₄⁺ as key species (Fig. 2). In addition, the sulphate factor includes minor contributions from elemental carbon and trace elements such as V, Rb, Ni and Br. This factor

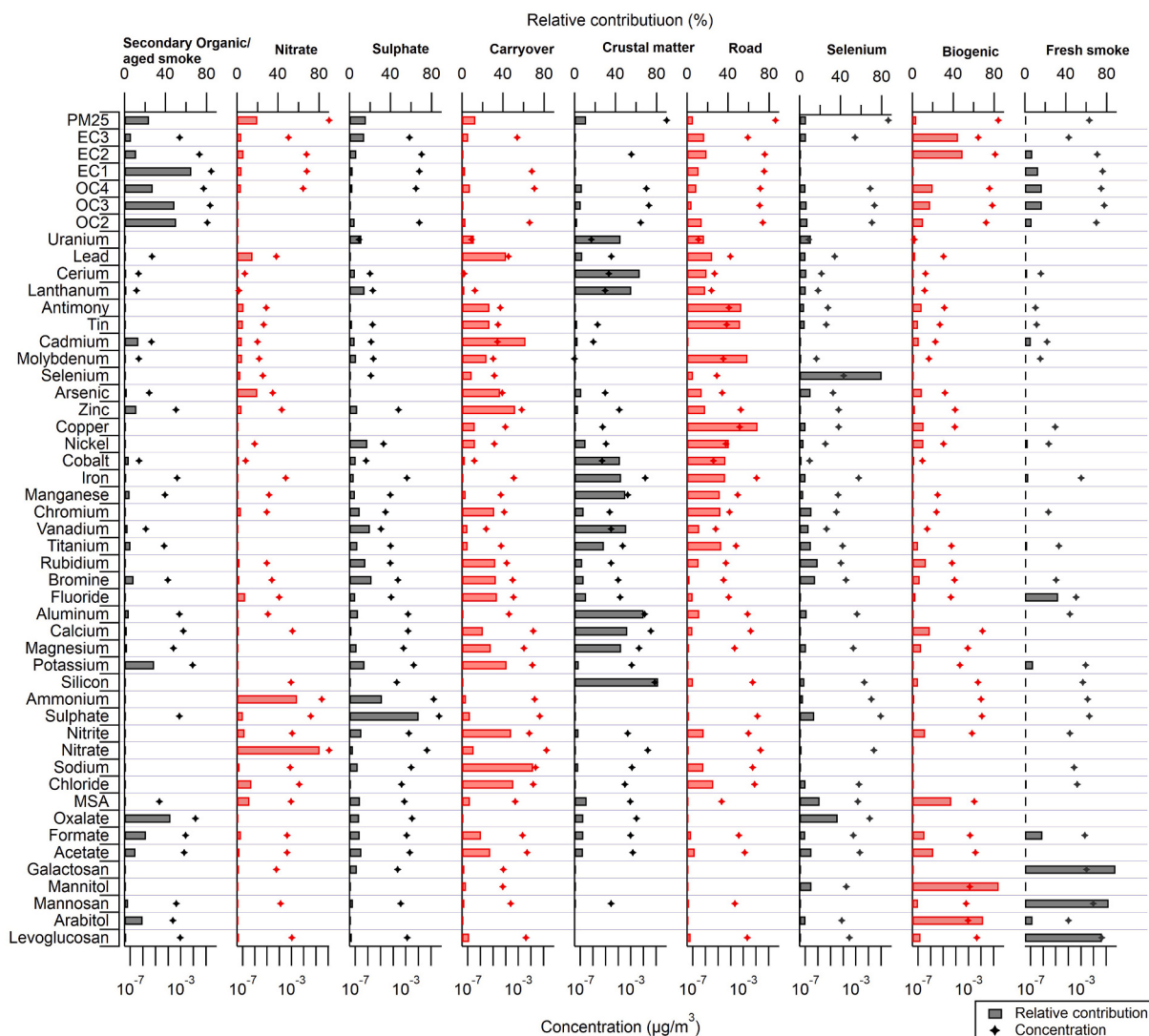


Fig. 2. Factor profiles for the multi-site 9 factor solution using data collected between February 2017 and March 2019 at the three Red Deer study sites (578 combined samples). Bars indicate relative contribution (top x-axis) and symbols indicate concentration (bottom x-axis). (For interpretation of the references to colour in this figure legend, the reader is referred to the web version of this article.)

makes up a notable contribution (16%) of total PM_{2.5}, with the largest seasonal mean contributions of 1.40–1.74 µg/m³ at the three stations in spring and seasonal mean contributions ranging between 0.72 and 1.13 µg/m³ in the other seasons (Fig. 3b). The sulphate factor episodes reach 24-hr average contributions of 2–6 µg/m³ and occur throughout the year. The Kruskal-Wallis test indicates that the factor contribution is consistent across all three sites, suggesting a regional influence. The CBPF analysis for the sulphate factor illustrates that elevated concentrations for all three sites were observed for winds from the east northeast to northeast direction, indicating a similar source area for all three sites (Fig. 6). The probability of elevated concentrations also increases with wind speed, suggesting that the sulphate factor likely has contributions from regional stack plumes (Uria-Tellaetxe and Carslaw, 2014). The CBPF analysis is, therefore, consistent with the possible impact from an electricity generating station located ~100 km to the northeast that emitted >9000 tonnes/year of SO₂ (Government of Canada, 2021). Regional concentrations of sulphate are also likely impacted by other SO₂ sources in the area, including a number of small (<550 tonnes/year) upstream oil and gas SO₂ sources throughout the region and another electricity generating station located ~150 km to the southeast of Red Deer (Government of Canada, 2021). The two electricity generating stations were coal-fired at the time of the study; one

has since switched to natural gas, and the other is in the process of changing fuel. As a result, SO₂ emissions and thus regional SO₄²⁻ are expected to decrease.

3.2.4. Carryover

The carryover factor includes the key components Na and Cd and notable contribution from Cl and Zn (Fig. 3) as well as the attribution of a number trace metals and elements. The carryover factor also contains 11% of NO₃⁻ mass and 8% of OC-4 and of SO₄²⁻ mass indicating marked contribution from secondary particulate matter.

The carryover factor makes a notable contribution (16%) to PM_{2.5}. At all three stations the highest seasonal means are in the winter (0.93–1.32 µg/m³) and the lowest in the summer (0.32–0.40 µg/m³). The carryover factor is the only factor with peak concentration in the winter, a season with a lower mixing height (Davies, 2012 and references within), the most frequent temperature inversions and stagnant conditions. Examples of mixing height values observed during periods of elevated contributions and relatively low contributions from the carryover factor are provided in the Supplementary Material (Figs. A 10 to 12). Temperature inversions likely contributed to the carryover factor. Emissions and other meteorological conditions facilitating the formation of secondary inorganic components also likely have a role.

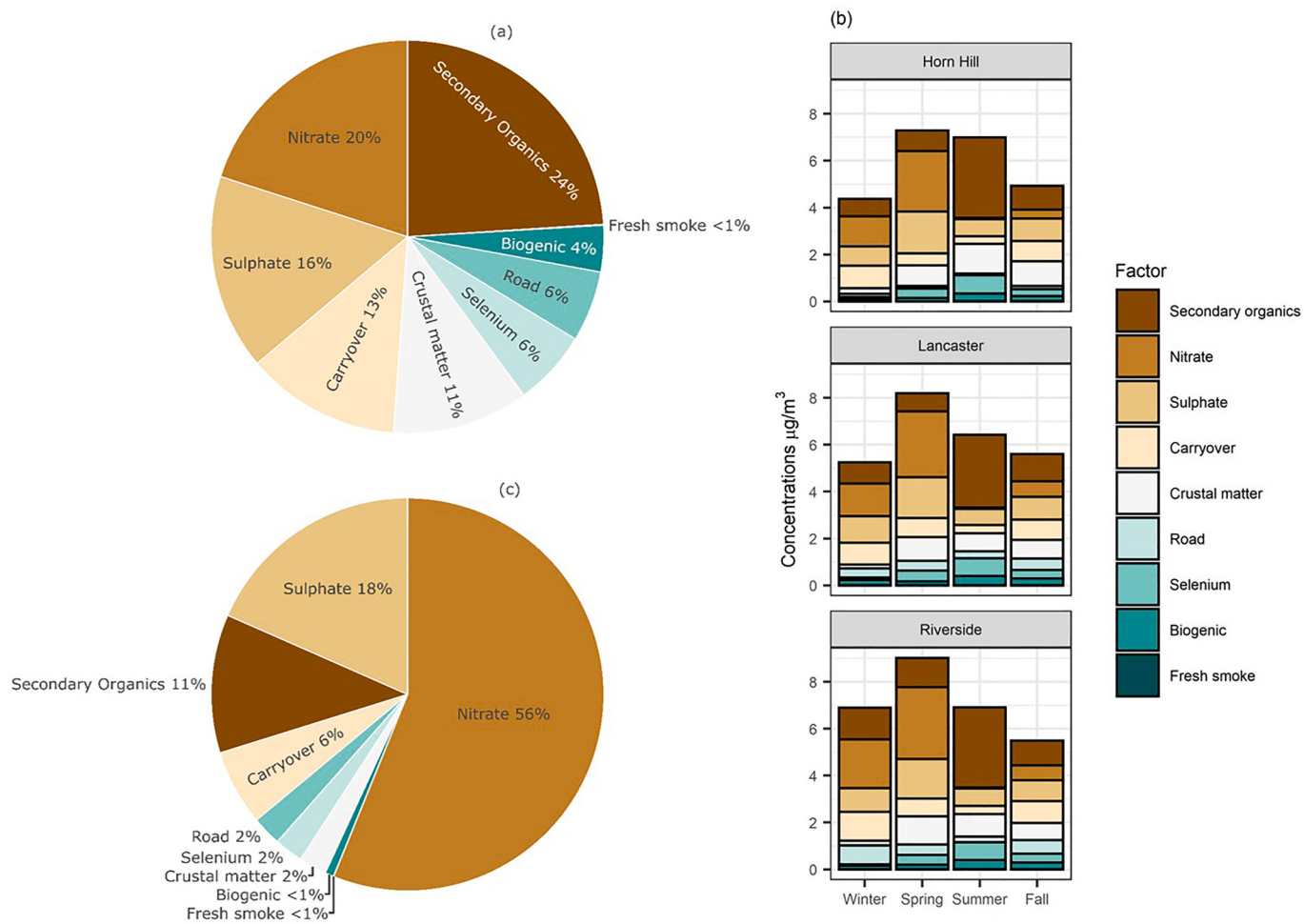


Fig. 3. The relative contribution of factors to PM_{2.5} mass at the three Red Deer study monitoring sites: (a) Study average relative contribution for data collected between February 2017 and March 2019 (578 combined samples), (b) average contribution by season and monitoring site for days with valid sample at all three monitoring sites (142 samples per site) and (c) relative contribution for samples collected between February 2017 and March 2019 (543 combined samples) with PM_{2.5} concentration $> 15 \mu\text{g}/\text{m}^3$ that were not impacted by wildfire smoke. (For interpretation of the references to colour in this figure legend, the reader is referred to the web version of this article.)

Similar contributions to measured PM_{2.5} mass concentrations are observed across all stations based on the Kruskal-Wallis test, largely driven by the strong seasonality of this factor. The CBPF analysis results did not indicate a common source area for the three sites (Fig. A6 in Supplementary material). For periods of elevated PM_{2.5} concentrations outside of wildfire-impacted days, this factor's contribution is reduced to 6% (Fig. 3c) thus has marginal contribution to periods of elevated PM_{2.5} in the study area.

3.2.5. Crustal matter

The crustal factor includes major contributions from silicon and aluminium, with minor contributions from other elements (Fig. 2), consistent with the composition of the earth's crustal matter. The crustal matter factor makes a moderate contribution (11%) to PM_{2.5}, with the largest seasonal mean contributions ($0.77\text{--}1.27 \mu\text{g}/\text{m}^3$) in the spring and summer (Fig. 3b). This factor's contribution to elevated concentration is reduced to 2% outside of wildfire impacted days, thus has minimal contribution to elevated concentrations leading to CAAQS exceedance.

In individual samples, the 24-hr average concentrations from the regional crustal matter factor can intermittently reach over $5 \mu\text{g}/\text{m}^3$. The contribution and variability of the crustal matter factor are consistent across stations based on the Kruskal-Wallis test, although concentrations are marginally higher at the rural station Horn Hill. CBPF analysis did not highlight a strong relationship (>0.2 probability) between the

crustal matter factor contributions and wind conditions (Fig. A7 in Supplemental information). Higher contributions for this factor are associated with drier conditions (higher temperatures and lower relative humidity) and moderate wind speed (5–10 km/hr) (Fig. 7). These conditions are consistent with dust, which is likely influenced by unpaved roads in the region and construction and agricultural activities.

3.2.6. Road

The road factor includes major contributions from Cu, Fe, and Mo, consistent with brake wear and other non-exhaust road traffic emissions (Thorpe and Harrison, 2008), and minor contributions from Na, Cl, likely from winter road de-icing (Fig. 2). The road factor comprises a small (6%) component of total PM_{2.5}. Contribution from this factor is highest in the winter months, likely due to increased contributions from winter road de-icing, traffic volume and lower boundary layer height typical during this season (Davies, 2012 and references within).

The road factor varies across the three stations, with study average contributions of $0.83 \mu\text{g}/\text{m}^3$ at Riverside, $0.40 \mu\text{g}/\text{m}^3$ at Lancaster, and $0.13 \mu\text{g}/\text{m}^3$ at Horn Hill. At the two urban stations (Riverside and Lancaster), 24-hr average contributions from the road factor were intermittent throughout the year, reaching $3 \mu\text{g}/\text{m}^3$ during some periods. At the rural Horn Hill station, contributions of the road factor were $<0.5 \mu\text{g}/\text{m}^3$ for all but three sample days. The Kruskal-Wallis test found a significant difference ($p \leq 0.05$) in the road factor between

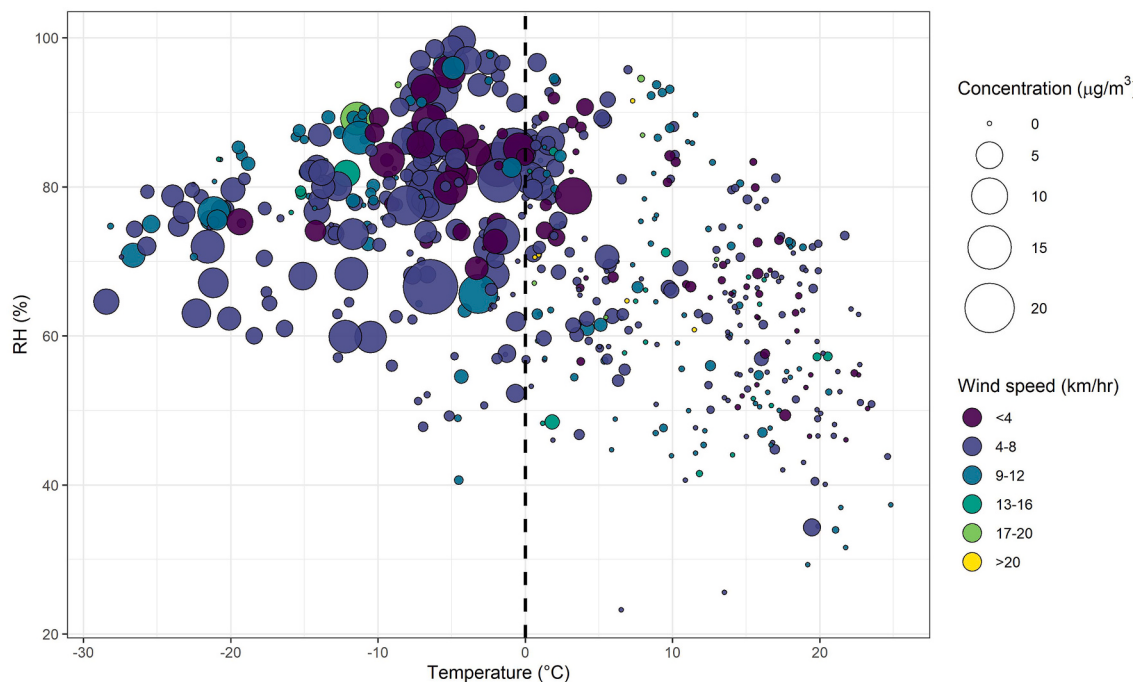


Fig. 4. Relationship between 24-hr average nitrate factor, relative humidity, wind speed and temperature for data collected between February 2017 and March 2019 at the three Red Deer study monitoring sites (578 combined samples). (For interpretation of the references to colour in this figure legend, the reader is referred to the web version of this article.)

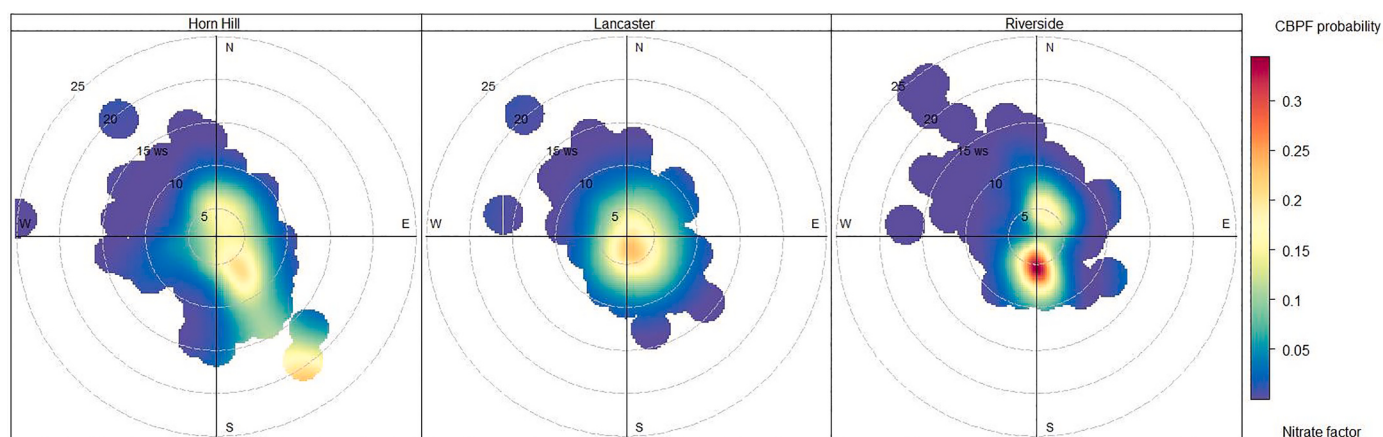


Fig. 5. CBPF for the nitrate factor when concentrations are above 75th percentile using all available data collected between February 2017 and March 2019 (Horn Hill: $n = 176$, Lancaster: $n = 142$ and Riverside: $n = 260$). 24-hr average wind speed and 24-hr vector average wind direction data were used. The assumption is that for a persistent and notable source, CBPF will illustrate a high probability when the sample site is downwind of the source.

stations. A pairwise Wilcox test (Core Development Team, 2021) found that Horn Hill was significantly different from Riverside and Lancaster stations (p -value < 0.01) but that there was not a significant difference between Riverside and Lancaster stations, suggesting similarities in contribution and periodicity of urban traffic emissions. CBPF analysis (Fig. 8) showed a relationship between elevated concentration at Riverside and wind speed and direction, with elevated concentrations observed for winds originating from the southwest. There are several major river crossings, including Highway 11, which crosses the river valley east-to-west and an urban downtown core a few km upstream of the station in a direction that aligns with the CBPF plot. At the Lancaster, located outside of the river valley, the relationship between the road factor and the wind directions is not as clear, suggesting a broad influence from various nearby roads. A weak probability was observed for southwesterly winds at Lancaster, is likely due to the distribution of

arterial roads with higher traffic counts to the southwest of the station. Figs. A 10 to 12 in the Supplementary Material illustrate examples of mixing height values observed during periods of elevated contributions and relatively low contributions from the road factor. Temperature inversions were likely one factor of many influencing contributions to the road factor.

The selenium factor includes the key species Se and oxalate, and also contains 14% of the SO_4^{2-} mass (Fig. 3). Se is typically associated with coal burning (Jeong et al., 2016; Laden et al., 2000). Various industrial activities emit Se in the study area, with coal-fired electricity-generating plants emitting both SO_2 and Se (Government of Canada, 2021). The selenium factor makes a small (6%) contribution to total $\text{PM}_{2.5}$, with the largest seasonal mean at the three sites in the summer (0.76–0.82 $\mu\text{g}/\text{m}^3$). 24-hr average concentrations $> 2 \mu\text{g}/\text{m}^3$ were periodically observed. Similar contributions and variability across sites are indicated

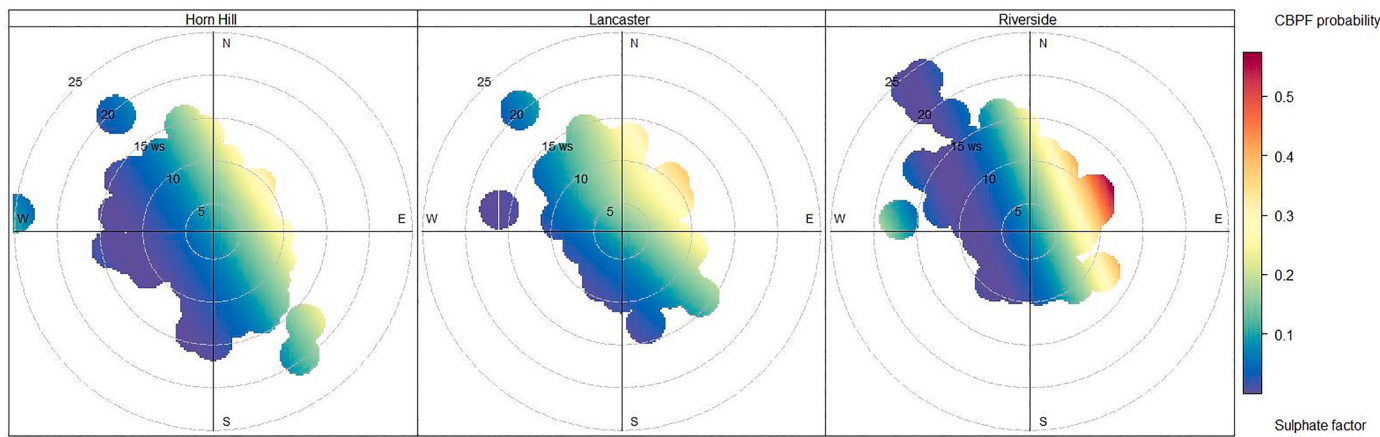


Fig. 6. CBPF for the sulphate factor when concentrations are above 75th percentile using all available data collected between February 2017 and March 2019 (Horn Hill: n = 176, Lancaster: n = 142 and Riverside: n = 260). 24-hr average wind speed and 24-hr vector average wind direction data were used. The assumption is that for a persistent and notable source, CBPF will illustrate a high probability when the sample site is downwind of the source.

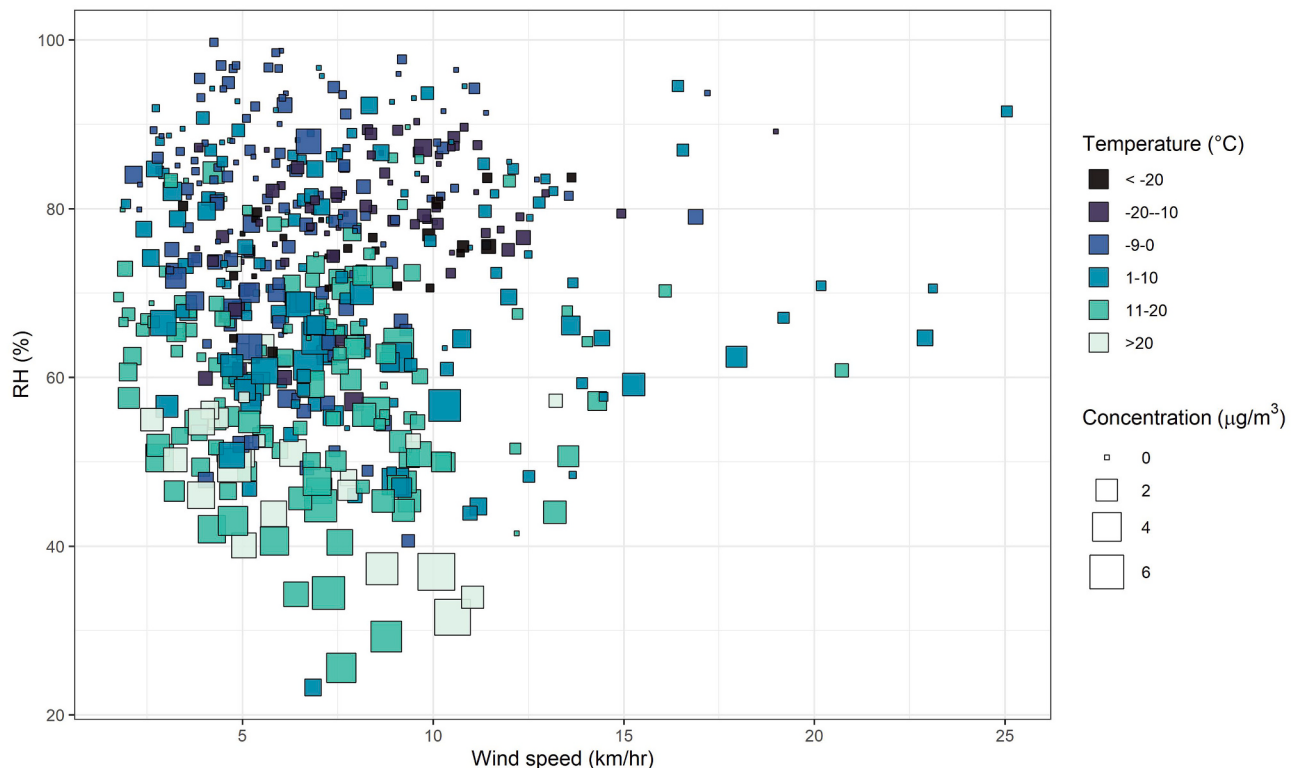


Fig. 7. Relationship between 24-hr average crustal matter factor contribution, relative humidity, wind speed and temperature for data collected between February 2017 and March 2019 at the three Red Deer study monitoring sites (578 combined samples). (For interpretation of the references to colour in this figure legend, the reader is referred to the web version of this article.)

by the Kruskal-Wallis test, suggesting that this factor is impacted by regional sources. The results of the CBPF analysis (Fig. A8 in Supplemental information) illustrate higher contributions for higher winds with an easterly component at the Lancaster and Horn Hill stations (southeastern at Lancaster and north-easterly at Horn Hill). This is consistent with a buoyant source, similar to the sulphate factor. The results for Riverside, located within the valley, also showed higher probably for easterly flows but also include higher contributions during periods of lower wind speeds, suggesting the within valley funnelling of transported air.

3.2.7. Biogenic

The biogenic factor includes major contributions from arabitol and mannitol and minor contributions from OC2–4, EC2–3, sulphate, silicon, and calcium (Fig. 2). Arabitol, mannitol and glucose can be used as primary biogenic organic matter indicators during the growing season (Bauer et al., 2008; Samaké et al., 2019). Emissions from vegetation include organic matter directly emitted by vegetation such as bacterial and fungal spores, or pollen, as well as the resuspension of plant debris. Much of this is in larger particle sizes, but a fraction can contribute to PM_{2.5} (Liang et al., 2013). During the study, the biogenic factor makes up a smaller contribution (4%) to PM_{2.5} mass concentration, with somewhat larger seasonal average in the summer (6%, 0.41 µg/m³) than

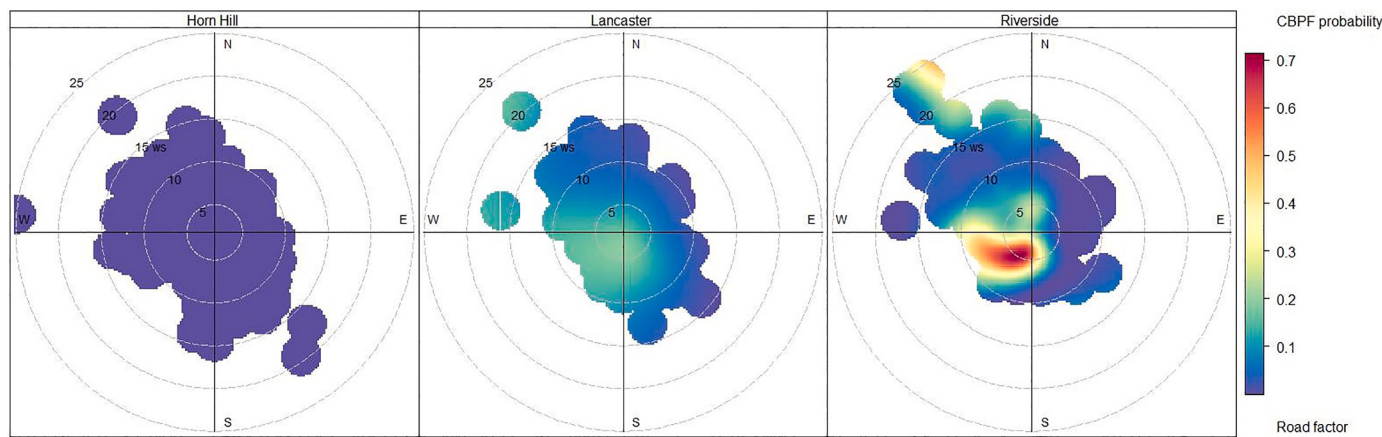


Fig. 8. CBPF for the road factor when concentrations are higher than 75th percentile using all available data collected between February 2017 and March 2019 (Horn Hill: n = 176, Lancaster: n = 142 and Riverside: n = 260). 24-hr average wind speed and 24-hr vector average wind direction data were used. The assumption is that for a persistent and notable source, CBPF will illustrate a high probability when the sample site is downwind of the source.

in other seasons (Fig. 3b). The presence of elemental carbon, sulphate and silicon indicates minor contributions from other regional sources. Significant differences ($p \leq 0.05$) in biogenic factor contributions between stations were found using the Kruskal-Wallis test. A pairwise Wilcoxon test indicated that contributions at the Horn Hill station were significantly different from the two sites in Red Deer (Riverside and Lancaster). This is consistent with Horn Hill's rural location, surrounded by crops and grassland. For the two sites that are outside of the Red Deer River valley, higher contributions for the biogenic factor are observed for winds with a westerly component (Fig. A9 in Supplemental Information).

3.2.8. Fresh smoke

The fresh smoke factor includes a larger contribution of levoglucosan, with a minor contribution from OC1, with a minimal presence of oxalate (Fig. 2), suggesting fresh smoke from wood biomass burning (Cubison et al., 2011; Hennigan et al., 2010). The relative abundance of anhydrosugars is affected by biomass burnt and the burn conditions. The levoglucosan/mannosan and mannosan/galactosan ratios of 5.25 and 3.59, respectively, suggest contributions from softwood combustion (Bhattarai et al., 2019 and citations within). The fresh smoke factor makes a very minor (< 1%) contribution to PM_{2.5} mass concentration. Although readily resolved as a stable factor, the contribution of this factor to 24-hr average PM_{2.5} ranged from 0.06 µg/m³ to below detection. Residential wood combustion is primarily recreational in the Red Deer area (e.g. fireplaces in the winter); the results indicate this activity

makes a very small contributor to PM_{2.5}. The Kruskal-Wallis test found a significant difference ($p \leq 0.05$) in contributions for the fresh smoke factor between stations, which is consistent with influences from local burning.

3.3. Cluster analysis results

The results of the hierarchical cluster analysis using data collected between February 2017 and March 2019 are shown in Fig. 9. 24-hr average station data and 24-hr integrated PM_{2.5} composition data are used in the comparison. There are two major branches in the cluster dendrogram. The branch on the left includes factors and parameters that are highest in the summertime. The branch on the right includes factors and parameters that have year-round or more significant winter and springtime components.

Within the left branch, the secondary organics/aged smoke and fresh smoke factors are clustered together, indicating some similarity between the temporal variability of these factors. The biogenic, crustal matter and selenium factors are clustered with 24-hr average temperature, daily total solar radiation and ozone, which is consistent with the summertime peaks of these factors. 24-hr average wind-speed, H₂S, and NH₃ are also clustered together in the left branch, although these were not closely associated with any of the factors.

Within the right branch, the two factors driven by secondary inorganic compounds, sulphate and nitrate, are clustered closely together. HNO₃ and SO₂ are in adjacent clusters, as expected since sulphate and

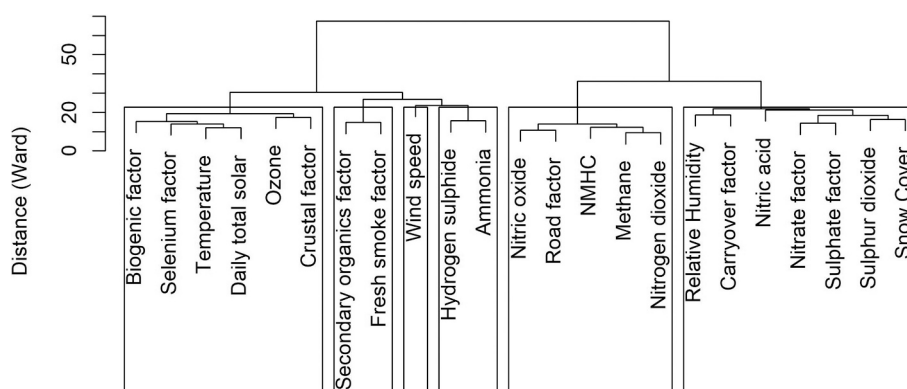


Fig. 9. Hierarchical clustering of PMF factors and 24-hr average co-monitored parameters and gases for data collected between February 2017 and March 2019 at the Red Deer Riverside station (260 samples). (For interpretation of the references to colour in this figure legend, the reader is referred to the web version of this article.)

nitrate factors have large contribution from sulphate and nitrate ions which form through gas-phase, heterogeneous and aqueous-phase oxidation of SO_2 and NO_2 (Seinfeld and Pandis, 2016). The right branch is also supported by the interdependent winter and springtime chemistry of sulphate, nitrate, HNO_3 and their precursor gases (Shah et al., 2018). This cluster, however, did not include NH_3 , implying that the formation of ammonium sulphate and nitrate is not ammonia-limited; this is explored further through thermodynamic modelling in Section 3.4. Snow cover and relative humidity are also in clusters adjacent to nitrate and sulphate, suggesting that higher concentrations of these factors are associated with snow cover and higher relative humidity. This is consistent with the observation that nitrate mass concentration increased on cold days (0 to -10°C) with relative humidity higher than 65% (Fig. 4). Similarly, Green et al. (2015) found cold days with snow cover, similar to the Red Deer area, were accompanied by higher relative humidity and an enhanced particle nitrate contribution in the Western United States. The carryover factor is also adjacent to the sulphate and nitrate factors. This is likely because the carryover factor contains 11% of NO_3^- (highest contribution outside of the nitrate factor) and 8% of the SO_4^{2-} (third highest contribution following the selenium factor) (Fig. 2) and therefore includes secondary inorganic particulate mass.

The road factor is clustered with NO, NO_2 , NMHC and methane, which is consistent with vehicle emissions. Furthermore, meteorological conditions, such as a stable boundary layer, could support the accumulation of vehicle emissions near the surface.

3.4. E-AIM modelling results

The sulphate and nitrate factors make up a significant portion of $\text{PM}_{2.5}$ at all three stations and are associated with anthropogenic sources that can be managed (i.e., relevant to the AQMS). During the study, the nitrate factor makes up 20%, and the sulphate factor makes up 16% of observed $\text{PM}_{2.5}$ (Fig. 3), with study average contributions of 56% and 18%, respectively, when $\text{PM}_{2.5}$ mass loadings exceed $15 \mu\text{g}/\text{m}^3$ outside of wildfire impact.

Using data collected between February 2017 and March 2019, thermodynamic modelling was used to determine whether the $\text{NO}_3-\text{SO}_4-\text{NH}_3$ system during the study was ammonia or nitric acid limited. This information can be used to determine the best air quality management strategy to reduce $\text{PM}_{2.5}$ associated with the nitrate and sulphate factors. The reaction of nitric acid and ammonia to form ammonium nitrate is more favourable at lower temperatures, higher relative humidity, and lower aerosol acidity (Seinfeld and Pandis, 2016). Depending on the relative concentrations of nitric acid and ammonia, as well as the meteorology, the formation of ammonium nitrate can either be nitric acid-limited or ammonia-limited and is reversible.

The efficacy of E-AIM was verified by comparing the E-AIM reconstructed moles of NH_4^+ , SO_4^{2-} , and NO_3^- to measured values. The slopes of a linear fit between modelled versus observed particle mole loadings vary between 1.05 and 1.07, with R^2 values from 0.985 to 0.993 (Figs. A13–15 in the Supplemental information). This shows that the inorganic aerosol system measured in Red Deer is in equilibrium and that E-AIM can be used to investigate the sensitivity of $\text{PM}_{2.5}$ mass loadings to changes in total nitrate and total ammonium.

The $\text{NO}_3(\text{T})$ ($\text{HNO}_3 + \text{NO}_3^-$) and NH_x ($\text{NH}_3 + \text{NH}_4^+$) model inputs were adjusted to -25% , -10% , $+10\%$, and $+25\%$ of the observed values. The resulting adjusted versus original E-AIM reconstructed (i.e., 0% adjusted) $\text{PM}_{2.5}$ ion mass are shown in Fig. 10 for the Riverside station. The results for Lancaster and Horn Hill are found in the Supplementary Information (Figs. A16–17). As shown in Fig. 10a, the concentrations of $\text{PM}_{2.5}$ ion mass are relatively insensitive to changes in total NH_x loadings. A 10% decrease in total NH_x only results in a $\sim 1\%$ reduction in ammonium nitrate and ammonium sulphate mass, whereas a 25% reduction yields a $\sim 7\%$ decrease. Additional total NH_x does not increase the $\text{PM}_{2.5}$ mass loadings.

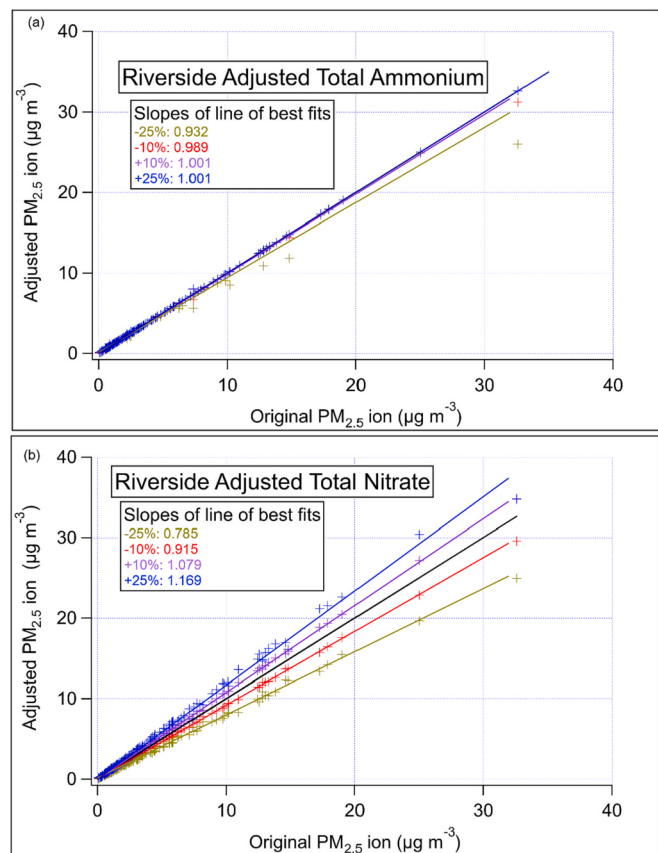


Fig. 10. Adjusted modelled concentrations of 24-hr average ammonium, sulphate, and nitrate ($\text{PM}_{2.5}$ ions) versus the original E-AIM reconstructed mass for data collected between February 2017 and March 2019 at the Red Deer Riverside station (260 samples). (For interpretation of the references to colour in this figure legend, the reader is referred to the web version of this article.)

Figure 10b shows that the aerosol system is much more sensitive to changes in $\text{NO}_3(\text{T})$. A 10% and 25% decrease in $\text{NO}_3(\text{T})$ result in a $\sim 9\%$ and $\sim 22\%$ decrease in $\text{PM}_{2.5}$ ion mass concentrations, respectively. The results for the Lancaster and Horn Hill sites are given in the Supplemental Information (Figs. A16–17) and are very similar to the Riverside site. These results imply that the $\text{NO}_3-\text{SO}_4-\text{NH}_3$ system in the region is nitric acid-limited. This is consistent with Fig. A18 which shows the observed mole loading of ammonia far exceeding the mole loading of nitric acid and the cluster analysis showing an association between nitrate, sulphate, and HNO_3 but no association to NH_3 . The amount of sulphate is insensitive to NH_x and $\text{NO}_3(\text{T})$ since it is non-volatile, unlike particulate ammonium and nitrate. However, the amount of sulphate affects ammonium and nitrate portioning since this process is sensitive to aerosol pH.

4. Conclusions

This study describes an investigation into the causes of a CAAQS $\text{PM}_{2.5}$ exceedance in Red Deer, and demonstrates an approach to narrow down potential $\text{PM}_{2.5}$ mitigation options when a region is affected by complex and varied emissions sources. $\text{PM}_{2.5}$ integrated samples were collected at three sites affected by different local emissions (one urban industrial site, one residential site, and one upwind site) between 2017 and 2019. The integrated $\text{PM}_{2.5}$ samples were analyzed for 57 components, which included metals, organic and elemental carbon and inorganic compounds. Due to the large number of samples from three sites and analyzed components, a robust PMF analysis that resolved nine factors was possible. The factors from the PMF analysis were interpreted

using CBPF and cluster analysis in order to assess influences such as local meteorological conditions and transport. In addition, a thermodynamic sensitivity analysis was performed to explore whether the observed ammonium nitrate is limited by HNO_3 or NH_3 . This study is the first multisite receptor source apportionment in Alberta, known to the authors, designed to explore regional and local sources and the limiting factor for the ammonia-sulphate-nitrate system.

Secondary formation of sulphate and nitrate were the dominant contributors to elevated $\text{PM}_{2.5}$ concentrations on days that were not affected by wildfire smoke. The sulphate factor CBPF analysis suggests notable power generation influence, though there are also ubiquitous smaller upstream oil and gas SO_2 sources in the region. Therefore, the contribution from the sulphate factor is expected to decrease alongside SO_2 emissions, as Alberta phases out coal-fired power generation (Government of Alberta, 2018). Observations from others (Balamurugan et al., 2022; Lin et al., 2020; Thunis et al., 2021; Womack et al., 2019) suggest that ongoing/planned reductions in SO_2 may not alone lead to marked decreases in $\text{PM}_{2.5}$, despite significant contributions of sulphate to total $\text{PM}_{2.5}$ mass. In future years, as the contribution from the sulphate factor decreases, the nitrate factor will likely become more dominant.

Therefore, mitigation options that target nitrate formation should be prioritized to manage $\text{PM}_{2.5}$ in the Red Deer area. The thermodynamic analysis showed that the ammonia-sulphate-nitrate system is HNO_3 limited for this study, suggesting NO_x emission reduction rather than NH_3 emission reduction as the most effective management tool. However, secondary $\text{PM}_{2.5}$ formation is non-linear. For example, Balamurugan et al. (2022) and Thunis et al. (2021) observed limited change in $\text{PM}_{2.5}$ mass concentrations when NO_2 decreased notably. They attributed this to increased ozone concentrations and thus increased contribution to $\text{PM}_{2.5}$ from heterogeneous reactions. This suggests that for some areas, emissions of VOCs with high ozone production potential must be reduced alongside NO_x in order to achieve $\text{PM}_{2.5}$ reductions. Small upstream oil and gas emission sources are ever-present in the study area and collectively contribute the most VOCs. Speciated VOC emissions information for the area is limited to large facilities. The most effective VOCs reductions should be targeted by determining the abundance of VOC species emitted by each type of industrial activity or emission source type and considering the VOC's OH reactivity.

Various types of local and regional sources contributed to the nitrate factor, as demonstrated by the CBPF analysis. Therefore, a regional air quality management approach would likely need to tackle multiple sources, focussing on NO_x and VOCs with high ozone production potential. In the Red Deer region, major NO_x and VOC emissions source sectors include non-industrial non-point sources, transportation, upstream oil and gas and electrical power generation. These emission sources are regulated by multiple jurisdictions, and as such would require a coordinated multi-jurisdictional emission management approach to further manage $\text{PM}_{2.5}$. Furthermore, public awareness campaigns and intermittent emissions management could target intermittent $\text{PM}_{2.5}$ episodes by focusing on meteorological conditions conducive to elevated nitrate concentrations.

CRediT authorship contribution statement

Yayne-abeba Aklilu: Writing – original draft, Conceptualization, Methodology, Formal analysis, Project administration. **Cristen Adams:** Writing – original draft, Conceptualization, Formal analysis. **Gregory R. Wentworth:** Writing – original draft, Formal analysis. **Maxwell Mazur:** Writing – review & editing, Resources. **Ewa Dabek-Zlotorzynska:** Writing – review & editing.

Declaration of Competing Interest

The authors declare that they have no known competing financial interests or personal relationships that could have appeared to influence the work reported in this paper.

Data availability

Data will be made available on request.

Acknowledgements

The authors would like to thank Parkland Air Management Zone and the Alberta Environment and Parks monitoring team for collecting integrated samples, operating monitoring sites and quality assurance and control of routinely collected gases and particulate mass data. The authors would like to thank Casandra Brown of Government of Alberta for providing data on wildfire impacted air quality samples and answering the authors many questions on the annual CAAQS assessment process and results. The authors would also like to gratefully acknowledge the major effort of the National Air Pollution Surveillance (NAPS) program of Environment and Climate Change Canada.

Appendix A. Supplementary data

Supplementary data to this article can be found online at <https://doi.org/10.1016/j.atmosres.2022.106583>.

References

- Al Mamun, A., Celo, V., Dabek-Zlotorzynska, E., Charland, J.P., Cheng, I., Zhang, L., 2021. Characterization and source apportionment of airborne particulate elements in the Athabasca oil sands region. *Sci. Total Environ.* 788, 147748. <https://doi.org/10.1016/j.scitotenv.2021.147748>.
- Alberta Electric System Operator, 2022. Alberta Electric System Operator: Current Supply Demand Report [online] Available from: http://ets.aeso.ca/ets_web/ip/Market/Reports/CSDReportServlet.
- Annesi-Maesano, I., Forastiere, F., Kunzli, N., Brunekreft, B., 2007. Particulate matter, science and EU policy. *Eur. Respir. J.* 29 (3), 428–431. <https://doi.org/10.1183/09031936.00129506>.
- Balamurugan, V., Chen, J., Qu, Z., Bi, X., Keutsch, F.N., 2022. Secondary PM Decreases Significantly Less Than NO₂ Emission Reductions During COVID Lockdown in Germany, 2, pp. 1–33.
- Bari, M.A., Kindzierski, W., 2016. B.: Fine particulate matter ($\text{PM}_{2.5}$) in Edmonton, Canada: source apportionment and potential risk for human health. *Environ. Pollut.* <https://doi.org/10.1016/j.envpol.2016.06.014>.
- Bari, M.A., Kindzierski, W., 2017. B.: Characteristics of air quality and sources affecting fine particulate matter ($\text{PM}_{2.5}$) levels in the City of Red Deer, Canada. *Environ. Pollut.* 221, 367–376. <https://doi.org/10.1016/j.envpol.2016.11.087>.
- Bauer, H., Claeys, M., Vermeylen, R., Schueller, E., Weinke, G., Berger, A., Puxbaum, H., 2008. Arabitol and mannitol as tracers for the quantification of airborne fungal spores. *Atmos. Environ.* 42 (3), 588–593. <https://doi.org/10.1016/j.atmosenv.2007.10.013>.
- Beck, H.E., Zimmermann, N.E., McVicar, T.R., Vergopolan, N., Berg, A., Wood, E.F., 2018. Present and future köppen-Geiger climate classification maps at 1-km resolution. *Sci. Data* 5, 1–12. <https://doi.org/10.1038/sdata.2018.214>.
- Belis, C.A., Karagulian, F., Larsen, B.R., Hopke, P.K., 2013. Critical review and meta-analysis of ambient particulate matter source apportionment using receptor models in Europe. *Atmos. Environ.* 69, 94–108. <https://doi.org/10.1016/j.atmosenv.2012.11.009>.
- Bhattarai, H., Saikawa, E., Wan, X., Zhu, H., Ram, K., Gao, S., Kang, S., Zhang, Q., Zhang, Y., Wu, G., Wang, X., Kawamura, K., Fu, P., Cong, Z., 2019. Levoglucosan as a tracer of biomass burning: recent progress and perspectives. *Atmos. Res.* 220 (November 2018), 20–33. <https://doi.org/10.1016/j.atmosres.2019.01.004>.
- Brown, C., 2019. Alberta: Air Zones Report 2015–2017. Government of Alberta, Ministry of Environment and Parks. ISBN 978-1-4601-4569-2. [online] Available from: <http://open.alberta.ca/dataset/f7fc0a13-02e4-4d2b-818a-357154868bee/resource/1144144a-c7a5-4a93-8c32-5dca3f195054/download/aep-alberta-air-zones-report-2015-2017.pdf>.
- Brown, C., 2021. Alberta Air Zones Report 2017–2019 [online] Available from: <http://open.alberta.ca/publications/alberta-air-zones-report-2017-2019>.
- Brown, C., Thi, A., Wentworth, G.R., 2022. Status of Air Quality in Alberta: Air Zones Report 2018–2020 [online] Available from: <https://open.alberta.ca/dataset/9b00aa-b3-c37d-4080-854e-5f329c621b92/resource/3afc6898-01d7-490b-bd76-02a6ed6e-dde3/download/aep-alberta-air-zones-report-2018-2020.pdf>.
- Brown, S.G., Eberly, S., Paatero, P., Norris, G.A., 2015. Methods for estimating uncertainty in PMF solutions: examples with ambient air and water quality data and guidance on reporting PMF results. *Sci. Total Environ.* 518–519, 626–635. <https://doi.org/10.1016/j.scitotenv.2015.01.022>.
- Carslaw, D.C., Ropkins, K., 2012. Openair — An R package for air quality data analysis. *Environ. Model. Softw.* 27–28, 52–61. <https://doi.org/10.1016/j.envsoft.2011.09.008>.
- CCME, 2019a. Guidance Document on Air Zone Management [online] Available from: http://www.ccme.ca/files/Resources/air/aqms/pn_1481_gdazm_e.pdf.

- CCME, 2019b. Guidance Document on Transboundary Flows and Exceptional Events for Air Zone Management [online] Available from: https://ccme.ca/en/res/guidancedocumentontransboundaryflowsandexceptionalevents_secured.pdf.
- City of Red Deer, 2022. When do We Salt and Sand? [online] Available from: <https://www.reddeer.ca/city-services/roads/snow-and-ice-program/how-it-works/when-do-we-salt-and-sand/>.
- Clegg, S.L., Brimblecombe, P., Wexler, A.S., 1998. Thermodynamic model of the system H₂-NH₄⁺-SO₄²⁻-NO₃⁻-H₂O at tropospheric temperatures. *J. Phys. Chem. A* 102 (12). <https://doi.org/10.1021/jp973042r>.
- Core Development Team, R.: A Language and Environment for Statistical Computing, R Found. Stat. Comput., vol. 2, <https://www.R-project.org> [online] Available from: <http://www.R-project.org>, 2021.
- Cropper, P.M., Bhardwaj, N., Overton, D.K., Hansen, J.C., Delbert, J., Cary, R.A., Kuprov, R., Baasandorj, M., 2019. Source apportionment analysis of winter (2016) Neil Armstrong academy data (West Valley city, Utah). *Atmos. Environ.* 116971, 2019. <https://doi.org/10.1016/j.atmosenv.2019.116971>.
- Cubison, M.J., Ortega, A.M., Hayes, P.L., Farmer, D.K., Day, D., Lechner, M.J., Brune, W.H., Apel, E., Diskin, G.S., Fisher, J.A., Fuelberg, H.E., Hecobian, A., Knapp, D.J., Mikoviny, T., Riemer, D., Sachse, G.W., Sessions, W., Weber, R.J., Weinheimer, A.J., Wisthaler, A., Jimenez, J.L., 2011. Effects of aging on organic aerosols from open biomass burning smoke in aircraft and laboratory studies. *Atmos. Chem. Phys.* 11 (23), 12049–12064. <https://doi.org/10.5194/acp-11-12049-2011>.
- Dabek-Zlotorzynska, E., Dann, T.F., Kalyani Martinelango, P., Celo, V., Brook, J.R., Mathieu, D., Ding, L., Austin, C., 2011. Canadian National Air Pollution Surveillance (NAPS) PM2.5 speciation program: methodology and PM2.5 chemical composition for the years 2003–2008. *Atmos. Environ.* 45 (3), 673–686. <https://doi.org/10.1016/j.atmosenv.2010.10.024>.
- Dai, Q., Hopke, P.K., Bi, X., Feng, Y., 2020. Improving apportionment of PM2.5 using multisite PMF by constraining G-values with a priori information. *Sci. Total Environ.* 736, 139657. <https://doi.org/10.1016/j.scitotenv.2020.139657>.
- Davies, M.J.E., 2012. Air quality modeling in the athabasca oil sands region. *Develop. Environ. Sci.* 11.
- Government of Alberta, 2014. Capital Region Science Report [online] Available from: <https://open.alberta.ca/dataset/51e77770-bf72-4851-8a6b-240d0f5b3856/resource/88698cff-7d86-4dc7-964a-4dc6d0433c04/download/2014-CapitalRegion-PM-ScienceReport-Dec2014.pdf>.
- Government of Alberta, 2015. Alberta: Air Zones Report 2011–2013 [online] Available from: <https://open.alberta.ca/dataset/a8e40aca-38f9-4493-aa66-fe4069169f17/resource/a4e0aaea-236d-4099-8ebb-003700a4a943/download/albertaairzonereport-2011-13-sep2015.pdf>.
- Government of Alberta, 2016. Red Deer Fine Particulate Matter Response Science Report [online] Available from: <https://open.alberta.ca/dataset/0477627b-0c6a-4b54-864a-9aa18a2e4162/resource/06d713c6-f96c-4605-9683-f40af9bd4ddd/download/reddeerfineparticulatescience-apr2016.pdf>.
- Government of Alberta, 2018. Transitioning Alberta to a Greener Grid, (September), 0–1 [online] Available from: www.alberta.ca/climate-coal-electricity.aspx.
- Government of Alberta, 2022. Alberta Acid Deposition Management Framework.
- Government of Canada, 2021. 2018 National Pollutant Release Inventory [online] Available from: <https://open.canada.ca/data/en/dataset/1fb7d8d4-7713-4ec6-b957-4a882a84fed3> (Accessed 18 February 2022).
- Government of Canada: Historical Climate Data, [online] Available from: <https://climate.weather.gc.ca/>, (n.d.).
- Green, M.C., Chow, J.C., Watson, J.G., Dick, K., Inouye, D., 2015. Effects of snow cover and atmospheric stability on winter PM2.5 concentrations in western U.S. Valleys. *J. Appl. Meteorol. Climatol.* 54 (6), 1191–1201. <https://doi.org/10.1175/JAMC-D-14-0191.1>.
- Gulia, S., Shiva Nagendra, S.M., Khare, M., Khanna, I., 2015. Urban air quality management—a review. *Atmos. Pollut. Res.* 6 (2), 286–304. <https://doi.org/10.5094/APR.2015.033>.
- Guo, H., Otjes, R., Schlag, P., Kiendler-Scharr, A., Nenes, A., Weber, R.J., 2018. Effectiveness of ammonia reduction on control of fine particle nitrate. *Atmos. Chem. Phys. Discuss.* 2018 (3), 1–31. <https://doi.org/10.5194/acp-2018-378>.
- Harpold, A.A., Brooks, P.D., 2018. Humidity determines snowpack ablation under a warming climate. *Proc. Natl. Acad. Sci. U. S. A.* 115 (6), 1215–1220. <https://doi.org/10.1073/pnas.1716789115>.
- Health Canada, 2021. Health Impacts of Air Pollution in Canada - Estimates of Premature Deaths and Nonfatal Outcomes. [online] Available from: <https://www.canada.ca/en/health-canada/services/publications/healthy-living/2021-health-effects-indoor-air-pollution.html#a3.3>.
- Heard, D.E., Carpenter, L.J., Creasey, D.J., Hopkins, J.R., Lee, J.D., Lewis, A.C., Pilling, M.J., Seakins, P.W., Carslaw, N., Emmerson, K.M., 2004. High levels of the hydroxyl radical in the winter urban troposphere. *Geophys. Res. Lett.* 31 (18) <https://doi.org/10.1029/2004GL020544>.
- Hennigan, C.J., Sullivan, A.P., Collett, J.L., Robinson, A.L., 2010. Levoglucosan stability in biomass burning particles exposed to hydroxyl radicals. *Geophys. Res. Lett.* 37 (9), 2–5. <https://doi.org/10.1029/2010GL043088>.
- Hopke, P.K., 2016. Review of receptor modeling methods for source apportionment. *J. Air Waste Manage. Assoc.* 66 (3), 237–259. <https://doi.org/10.1080/10962247.2016.1140693>.
- Jeong, C.-H., Wang, J., Evans, G., 2016. Source apportionment of urban particulate matter using hourly resolved trace metals, organics, and inorganic aerosol components. *Atmos. Chem. Phys. Discuss.* 0 (April), 1–32. <https://doi.org/10.5194/acp-2016-189>.
- Koenig, J.Q., 2000. Health Effects of Particulate Matter. In: *Health Effects of Ambient Air Pollution*. Springer US, Boston, MA, pp. 115–137.
- Kroll, J.H., Lim, C.Y., Kessler, S.H., Wilson, K.R., 2015. Heterogeneous oxidation of atmospheric organic aerosol: kinetics of changes to the amount and oxidation state of particle-phase organic carbon. *J. Phys. Chem. A* 119 (44), 10767–10783. <https://doi.org/10.1021/acs.jpca.5b06946>.
- Laden, F., Neas, L.M., Dockery, D.W., Schwartz, J., 2000. Association of fine particulate matter from different sources with daily mortality in six U.S. cities. *Environ. Health Perspect.* 108 (10), 941–947. <https://doi.org/10.1289/ehp.00108941>.
- Landis, M.S., Patrick Pancras, J., Graney, J.R., White, E.M., Edgerton, E.S., Legge, A., Percy, K.E., 2017. Source apportionment of ambient fine and coarse particulate matter at the Fort McKay community site, in the Athabasca Oil Sands Region, Alberta, Canada. *Sci. Total Environ.* 584–585, 105–117. <https://doi.org/10.1016/j.scitotenv.2017.01.110>.
- Landis, M.S., Edgerton, E.S., White, E.M., Wentworth, G.R., Sullivan, A.P., Dillner, A.M., 2018. The impact of the 2016 Fort McMurray Horse River Wildfire on ambient air pollution levels in the Athabasca Oil Sands Region, Alberta, Canada. *Sci. Total Environ.* 618, 1665–1676. <https://doi.org/10.1016/j.scitotenv.2017.10.008>.
- Lee, S., Liu, W., Wang, Y., Russell, A.G., Edgerton, E.S., 2008. Source apportionment of PM 2.5: Comparing PMF and CMB results for four ambient monitoring sites in the southeastern United States. *Atmos. Environ.* 42 (18), 4126–4137. <https://doi.org/10.1016/j.atmosenv.2008.01.025>.
- Liang, L., Engling, G., He, K., Du, Z., Cheng, Y., Duan, F., 2013. Evaluation of fungal spore characteristics in Beijing, China, based on molecular tracer measurements. *Environ. Res. Lett.* 8 (1) <https://doi.org/10.1088/1748-9326/8/1/014005>.
- Lin, Y., Zhang, Y., Fan, M., Bao, M., 2020. Heterogeneous formation of particulate nitrate under ammonium-rich regimes during the high-PM_{2.5} events in Nanjing, China. *Atmos. Chem. Phys.* 20 (6), 3999–4011. <https://doi.org/10.5194/acp-20-3999-2020>.
- May, A.A., Nguyen, N.T., Presto, A.A., Gordon, T.D., Lipsky, E.M., Karve, M., Gutierrez, A., Robertson, W.H., Zhang, M., Brandow, C., Chang, O., Chen, S., Cicero-Fernandez, P., Dinkins, L., Fuentes, M., Huang, S.M., Ling, R., Long, J., Maddox, C., Massetti, J., McCauley, E., Miguel, A., Na, K., Ong, R., Pang, Y., Rieger, P., Sax, T., Truong, T., Vo, T., Chattopadhyay, S., Maldonado, H., Maricq, M.M., Robinson, A.L., 2014. Gas- and particle-phase primary emissions from in-use, on-road gasoline and diesel vehicles. *Atmos. Environ.* 88, 247–260. <https://doi.org/10.1016/j.atmosenv.2014.01.046>.
- Murphy, J.G., Gregoire, P.K., Tevilin, A.G., Wentworth, G.R., Ellis, R.A., Markovic, M.Z., VandenBoer, T.C., 2017. Observational constraints on particle acidity using measurements and modelling of particles and gases. *Faraday Discuss.* <https://doi.org/10.1039/c7fd00086c>.
- Paatero, P., 1997. Least squares formulation of robust non-negative factor analysis. *Chemom. Intell. Lab. Syst.* 37 (1), 23–35. [https://doi.org/10.1016/S0169-7439\(96\)00044-5](https://doi.org/10.1016/S0169-7439(96)00044-5).
- Pandolfi, M., Mooibroek, D., Hopke, P., van Pinxteren, D., Querol, X., Herrmann, H., Alastuey, A., Favez, O., Hüglin, C., Perdriz, E., Riffault, V., Sauvage, S., van der Swaluw, E., Tarasova, O., Colette, A., 2019. Long range and local air pollution: what can we learn from chemical speciation of particulate matter at paired sites? *Atmos. Chem. Phys. Discuss.* 1–49 <https://doi.org/10.5194/acp-2019-493>.
- Parworth, C.L., Young, D.E., Kim, H., Zhang, X., Cappa, C.D., Collier, S., Zhang, Q., 2017. Wintertime water-soluble aerosol composition and particle water content in Fresno, California. *J. Geophys. Res.* 122 (5), 3155–3170. <https://doi.org/10.1002/2016JD026173>.
- Samaké, A., Jaffrezo, J.L., Favez, O., Weber, S., Jacob, V., Canete, T., Albinet, A., Charron, A., Riffault, V., Perdriz, E., Waked, A., Golly, B., Salameh, D., Chevrier, F., Miguel Oliveira, D., Besomes, J.L., Martins, J.M.F., Bonnaire, N., Conil, S., Guillaud, G., Mesbah, B., Rocq, B., Robic, P.Y., Hulin, A., Le Meur, S., Descheemaeker, M., Chretien, E., Marchand, N., Uzu, G., 2019. Arabitol, mannitol, and glucose as tracers of primary biogenic organic aerosol: the influence of environmental factors on ambient air concentrations and spatial distribution over France. *Atmos. Chem. Phys.* 19 (16), 11013–11030. <https://doi.org/10.5194/acp-19-11013-2019>.
- Seinfeld, J.H., Pandis, S.N., 2016. *Atmospheric Chemistry and Physics: From Air Pollution to Climate Change*.
- Shah, V., Jaeglé, L., Thornton, J.A., Lopez-Hilfiker, F.D., Lee, B.H., Schroder, J.C., Campuzano-Jost, P., Jimenez, J.L., Guo, H., Sullivan, A.P., Weber, R.J., Green, J.R., Fiddler, M.N., Billilign, S., Campos, T.L., Stell, M., Weinheimer, A.J., Montzka, D.D., Brown, S.S., 2018. Chemical feedbacks weaken the wintertime response of particulate sulfate and nitrate to emissions reductions over the eastern United States. *Proc. Natl. Acad. Sci. U. S. A.* 115 (32), 8110–8115. <https://doi.org/10.1073/pnas.1803295115>.
- Statistics Canada: Households and the Environment, (vol. 11) [online] Available from: <https://www15.statcan.gc.ca/n1/en/pub/11-526-s/11-526-s2013002-eng.pdf?st=621dzUp>, 2011.
- Sun, J., Liu, L., Xu, L., Wang, Y., Wu, Z., Hu, M., Shi, Z., Li, Y., Zhang, X., Chen, J., Li, W., 2018. Key role of nitrate in phase transitions of urban particles: implications of important reactive surfaces for secondary aerosol formation. *J. Geophys. Res. Atmos.* 123 (2), 1234–1243. <https://doi.org/10.1002/2017JD027264>.
- Tao, Y., Murphy, J.G., 2019. Evidence for the importance of semivolatile organic ammonium salts in ambient particulate matter. *Environ. Sci. Technol.* 53 (1), 108–116. <https://doi.org/10.1021/acs.est.8b03800>.
- Thorpe, A., Harrison, R.M., 2008. Sources and properties of non-exhaust particulate matter from road traffic: a review. *Sci. Total Environ.* 400 (1–3), 270–282. <https://doi.org/10.1016/j.scitotenv.2008.06.007>.
- Thunis, P., Clappier, A., Beekmann, M., Putaud, J.P., Cuvelier, C., Madrazo, J., De Meij, A., 2021. Non-linear response of PM_{2.5} to changes in NO_x and NH₃ emissions in the Po basin (Italy): Consequences for air quality plans. *Atmos. Chem. Phys.* 21 (12), 9309–9327. <https://doi.org/10.5194/acp-21-9309-2021>.

- Uria-Tellaetxe, I., Carslaw, D.C., 2014. Conditional bivariate probability function for source identification. Environ. Model. Softw. 59, 1–9. <https://doi.org/10.1016/j.envsoft.2014.05.002>.
- US-EPA, 2014. EPA Positive Matrix Factorization (PMF)5.0 Fundamentals.
- Wexler, A.S., Clegg, S.L., 2002. Atmospheric aerosol models for systems including the ions H⁺, NH4⁺, Na⁺, SO42-, NO₃-, Cl⁻, Br⁻, and H2O. J. Geophys. Res. Atmos. <https://doi.org/10.1029/2001JD000451>.
- Womack, C.C., McDuffie, E.E., Edwards, P.M., Bares, R., de Gouw, J.A., Docherty, K.S., Dubé, W.P., Fibiger, D.L., Franchin, A., Gilman, J.B., Goldberger, L., Lee, B.H., Lin, J. C., Long, R., Middlebrook, A.M., Millet, D.B., Moravek, A., Murphy, J.G., Quinn, P. K., Riedel, T.P., Roberts, J.M., Thornton, J.A., Valin, L.C., Veres, P.R., Whitehill, A. R., Wild, R.J., Warneke, C., Yuan, B., Baasandorj, M., Brown, S.S., 2019. An Odd oxygen framework for wintertime ammonium nitrate aerosol pollution in urban areas: NOx and VOC control as mitigation strategies. Geophys. Res. Lett. 46 (9), 4971–4979. <https://doi.org/10.1029/2019GL082028>.
- Xing, Y.F., Xu, Y.H., Shi, M.H., Lian, Y., 2016. X: the impact of PM2.5 on the human respiratory system. J. Thorac. Dis. 8 (1), E69–E74. <https://doi.org/10.3978/j.issn.2072-1439.2016.01.19>.